

**EFFECTS OF LOADING RATES ON COMPRESSIVE
STRENGTH OF SANDSTONES**

Numchok Kenkhunthod

**A Thesis Submitted in Partial Fulfillment of the Requirements
for the Degree of Master of Engineering in Geotechnolgy**

Suranaree University of Technology

Academic Year 2009

ผลกระทบของอัตราการกดต่อกำลังรับแรงกดของหินทราย

นายนำโชค เกณฑ์ขุนทด

วิทยานิพนธ์นี้เป็นส่วนหนึ่งของการศึกษาตามหลักสูตรปริญญาวิศวกรรมศาสตรมหาบัณฑิต
สาขาวิชาเทคโนโลยีธรณี
มหาวิทยาลัยเทคโนโลยีสุรนารี
ปีการศึกษา 2552

**EFFECTS OF LOADING RATES ON COMPRESSIVE
STRENGTH OF SANDSTONES**

Suranaree University of Technology has approved this thesis submitted in partial fulfillment of the requirements for a Master's Degree.

Thesis Examining Committee

(Asst. Prof. Thara Lekuthai)

Chairperson

(Assoc. Prof. Dr. Kittitap Fuenkajorn)

Member (Thesis Advisor)

(Dr. Prachya Tepnarong)

Member

(Prof. Dr. Pairote Sattayatham)

Acting Vice Rector for Academic Affairs

(Assoc. Prof. Dr. Vorapot Khompis)

Dean of Institute of Engineering

นำโชค เกษท์ขุนทด : ผลกระทบของอัตราการกดต่อกำลังรับแรงกดของหินทราย
(EFFECTS OF LOADING RATES ON COMPRESSIVE STRENGTH OF
SANDSTONES) อาจารย์ที่ปรึกษา : รองศาสตราจารย์ ดร. กิตติเทพ เฟื่องขจร,
65 หน้า

ผลกระทบของอัตราการกดต่อค่ากำลังกดสูงสุดและค่าสัมประสิทธิ์ความยืดหยุ่นของหินได้ถูกตระหนักถึงมาเป็นเวลานาน ค่ากำลังกดสูงสุดของหินจะลดลงตามอัตราการกดสิ่งที่น่าสนใจเป็นห่วงประการหนึ่งคือการนำคุณสมบัติของหินที่ทดสอบได้ในห้องปฏิบัติการมาประยุกต์ใช้ในการออกแบบและประเมินเสถียรภาพของหินในภาคสนาม กล่าวคือคุณสมบัติของหินที่ทดสอบได้ในห้องปฏิบัติการภายใต้อัตราการกดที่ค่อนข้างสูงนั้น(ประมาณ 0.5-1 เมกกะปาสกาลต่อวินาที ซึ่งถูกกำหนดโดย ASTM) จะสูงกว่าอัตราการกดในมวลหินที่รองรับโครงสร้างทางวิศวกรรมในระหว่างการก่อสร้าง ข้อแตกต่างระหว่างคุณสมบัติของหินที่ได้จากห้องปฏิบัติการและคุณสมบัติของหินที่แท้จริงในภาคสนามจะขึ้นกับชนิดของหินนั้น คุณลักษณะในการกดและระยะเวลาการก่อสร้างของโครงการ

วัตถุประสงค์ของงานวิจัยนี้คือเพื่อศึกษาในเชิงการทดสอบของผลกระทบของอัตราการกดต่อค่าความแข็งของหินทราย 3 ชนิดและเพื่อพัฒนาเกณฑ์การแตกที่มีตัวแปรจากผลกระทบของอัตราการกดเข้ามาพิจารณาด้วย การทดสอบประกอบด้วย การกดในแกนเดียว การกดในสามแกนและการกดโดยการเพิ่มขึ้นของแรงกดแบบขึ้นบันไดโดยมีการควบคุมอัตราการกดอย่างแม่นยำ การทดสอบดังกล่าวดำเนินการเพื่อศึกษาผลกระทบของอัตราการกดต่อความแข็งและความเหนียวของตัวอย่างหินทราย ความเค้นในแนวแกนที่ให้บนตัวอย่างหินจะมีอัตราการกดที่คงที่ในระดับต่างกันเริ่มต้นที่ 0.001 0.01 0.1 1.0 ไปจนถึง 10 เมกกะปาสกาลต่อวินาที ความเค้นรอบข้างของตัวอย่างหินจะผันแปรจาก 0 3 7 ไปจนถึง 12 เมกกะปาสกาล ผลที่ได้ระบุว่าค่าความแข็งและความยืดหยุ่นของตัวอย่างหินทรายจะเพิ่มขึ้นตามอัตราการกด ผลกระทบนี้ดูเหมือนไม่ขึ้นกับความเค้นรอบข้าง เพื่อที่จะพิจารณาความเค้นในสามแกนที่จุดแตกค่าความยืดหยุ่นของหินจึงถูกกำหนดให้เป็นฟังก์ชันของอัตราของความเค้นที่ไม่ผันแปร (dI_2/dt) สมมุติในที่นี้ว่าพลังงานที่ทำให้หินแต่ละชนิดแตกจะไม่ขึ้นกับอัตราการกด ดังนั้นเกณฑ์การแตกในสามแกนสามารถถูกพัฒนาบนพื้นฐานของพลังงานความเครียด โดยมีการพิจารณาความแข็งและความเหนียวของหินที่อยู่ในฟังก์ชันของอัตราการกด ค่าพลังงานความเครียดเบี่ยงเบน (W_p) ถูกกำหนดให้อยู่ในฟังก์ชันของความเค้นเฉลี่ย (σ_m) ซึ่งพบว่าสมการดังกล่าวสอดคล้องกับความแข็งแรงของหินทรายในช่วงอัตราการกดที่ทดสอบใน งานวิจัยนี้

เกณฑ์การแตกที่เสนอมาในงานวิจัยนี้มีประโยชน์ในการใช้คาดคะเนความแข็งแกร่งและการเปลี่ยนรูปร่างของหินในภาคสนามที่อยู่ภายใต้อัตราการกดที่แตกต่างไปจากอัตราการกดที่ใช้ในห้องปฏิบัติการ

NUMCHOK KENKHUNTHOD : EFFECTS OF LOADING RATES ON
COMPRESSIVE STRENGTH OF SANDSTONES. THESIS ADVISOR :
ASSOC. PROF. KITTITEP FUENKAJORN, Ph.D., PE., 65 PP.

LOADING RATE/COMPRESSIVE STRENGTH/CONFINING PRESSURE/
SANDSTONE/QUASI-STATIC.

The effects of loading rate on the compressive strength and elastic modulus of rocks have long been recognized. It has been found that rock compressive strength decreases with the loading rate. A primary concern of this effect arises when one applies the laboratory-determined properties of intact rock in the design and stability analysis of rock under in-situ conditions. The strength properties obtained from laboratory testing under a relatively high loading rate (normally about 0.5-1.0 MPa per second as specified by the American Society for Testing and Materials – ASTM) tend to be greater than those of the geologic structures during constructions. The discrepancy between the laboratory-determined properties and the actual in-situ properties also depends on rock types, loading characteristics and the project duration.

The objectives of this research are to experimentally assess the effect of loading rate on the compressive strength of three types of sandstone and to derive a strength criterion that explicitly incorporates the loading effect. Rate-controlled uniaxial, rate-controlled triaxial compressive strength tests and quasi-static loading tests have been performed to assess the loading rate effects on the strength and stiffness of sandstone specimens. The applied axial stresses are controlled at constant rates of 0.001, 0.01, 0.1, 1.0 and 10 MPa/s. The confining pressures are varied from 0, 3, 7 to 12 MPa. The sandstone strengths and elastic moduli tend to increase exponentially

with the loading rates. The effects seem to be independent of the confining pressures. To consider all three principal stresses at failure the rock stiffness is defined as a function of the rate of the second order of stress invariant ($\partial J_2/\partial t$). Assuming that the energy required to fail the specimen for each rock type is independent of the applied loading rate, a multi-axial strength criterion based on the strain energy density is developed by taking into consideration the rate-dependent strength and stiffness of the rock. The distortional strain energy density (W_d) defined as a function of mean stress (σ_m) can well describe the sandstone strengths within the range of the loading rates tested here. The proposed strength criterion is useful for predicting the strength and deformation characteristics of in-situ rocks subject to loading rates that are different from those used in the laboratory.

School of Geotechnology

Academic Year 2009

Student's Signature _____

Advisor's Signature _____

ACKNOWLEDGMENTS

I wish to acknowledge the funding support of Suranaree University of Technology (SUT).

I would like to express my sincere thanks to Assoc. Prof. Dr. Kittitip Fuenkajorn, thesis advisor, who gave a critical review and constant encouragement throughout the course of this research. Further appreciation is extended to Asst. Prof. Thara Lekuthai : Chairman, School of Geotechnology and Dr. Prachya Tepnarong, School of Geotechnology, Suranaree University of Technology who are member of my examination committee. Grateful thanks are given to all staffs of Geomechanics Research Unit, Institute of Engineering who supported my work.

Finally, I most gratefully acknowledge my parents and friends for all their supported throughout the period of this research.

Numchok Kenkhunthod

TABLE OF CONTENTS

	Page
ABSTRACT (THAI)	I
ABSTRACT (ENGLISH)	III
ACKNOWLEDGEMENTS	V
TABLE OF CONTENTS	VI
LIST OF TABLES	IX
LIST OF FIGURES	X
LIST OF SYMBOLS AND ABBREVIATIONS.....	XIII
CHAPTER	
I INTRODUCTION.....	1
1.1 Background and rationale.....	1
1.2 Research objectives	2
1.3 Scope and limitations	2
1.4 Research methodology	3
1.4.1 Literature review	4
1.4.2 Sample collection and preparation	4
1.4.3 Laboratory testing	4
1.4.3.1 Uniaxial compressive strength tests	5
1.4.3.2 Quasi-static loading tests.....	5
1.4.3.3 Triaxial compressive strength tests	5

TABLE OF CONTENTS (Continued)

	Page
1.4.4 Development of mathematical relations	6
1.4.5 Thesis writing	6
1.5 Thesis contents	6
II LITERATURE REVIEW	7
III SAMPLE PREPARATION	15
3.1 Introduction	15
3.2 Sample preparation.....	15
IV LABORATORY EXPERIMENT.....	22
4.1 Introduction.....	22
4.2 Rate-controlled uniaxial compressive strength tests (UCS)	22
4.3 Quasi-static loading tests.....	23
4.4 Rate-controlled triaxial compressive strength tests.....	24
4.5 Test results	26
V DEVELOPMENT OF STRENGTH CRITERIA	36
5.1 Introduction.....	36
5.2 Multi-axial strength criterion for triaxial testing.....	36
5.3 A rate-dependent strength criterion.....	39
5.4 Strength criterion based on strain energy density	41
VI DISCUSSIONS CONCLUSIONS AND RECOMMENDATIONS FOR FUTURE STUDIES.....	45

TABLE OF CONTENTS (Continued)

	Page
6.1 Discussions and conclusions.....	45
6.2 Recommendations for future studies.....	46
REFERENCES.....	47
APPENDIX A TECHNICAL PUBLICATION	51
BIOGRAPHY	65

LIST OF TABLES

Table	Page
4.1 Summary of test results of Phra Wihan sandstone.....	27
4.2 Summary of test results of Phu Phan sandstone	28
4.3 Summary of test results of Phu Kradung sandstone	29
5.1 Strength calculation in terms of $J_2^{1/2}$ and σ_m on Phra Wihan sandstone.....	38
5.2 Strength calculation in terms of $J_2^{1/2}$ and σ_m on Phu Phan sandstone	39
5.3 Strength calculation in terms of $J_2^{1/2}$ and σ_m on Phu Kradung sandstone.....	40

LIST OF FIGURES

Figure	Page
1.1 Research methodology.....	3
2.1 The relationships between the residual (irreversible) axial $\Delta\varepsilon_1$ and lateral $\Delta\varepsilon_2$ strains.....	13
2.2 The relationships of stress-strain	14
3.1 Sandstones blocks with nominal size of 10 cm x 20 cm x 40 cm are collected from Saraburi province.....	16
3.2 Laboratory core drilling of PK sandstone.....	17
3.3 A core specimen of PK sandstone is cut by a cutting machine	18
3.4 PK, PP and PW sandstones specimens prepared for the uniaxial compressive strength test.....	19
3.5 PW, PP and PK sandstones specimens for the quasi-static test.....	20
3.6 The rectangular block specimens of PW, PP and PK sandstones used in the polyaxial testing are cut and ground	21
4.1 A cylindrical specimen for PW sandstone is tested under rate-controlled uniaxial compression	23
4.2 A cylindrical specimen for PK sandstone is tested under quasi-static loading.....	24
4.3 A polyaxial load frame used for the rate-controlled triaxial compressive strength tests.....	25

LIST OF FIGURES (Continued)

Figure	Page
4.4 Uniaxial compressive strength and quasi-static testing result under loading rates varied from 0.001, 0.01, 0.1 and 1.0 MPa/s, for PW, PP and PK sandstones.....	30
4.5 Examples of triaxial compressive strength testing results for PW sandstone with axial loading rates of 1, 0.1, and 0.01 MPa/s (from top to bottom).....	31
4.6 Examples of triaxial compressive strength testing results for PP sandstone with axial loading rates of 1, 0.1, and 0.01 MPa/s (from top to bottom).....	32
4.7 Examples of triaxial compressive strength testing results for PK sandstone with axial loading rates of 1, 0.1, and 0.01 MPa/s (from top to bottom).....	33
4.8 Elastic modulus (E) as a function of applied loading rate ($\partial\sigma_1/\partial t$) for PW, PP and PK sandstones	34
4.9 Maximum principal stress (σ_1) as a function of minimum principal stress (σ_3) at failure various loading rates for PW, PP and PK sandstones	35
5.1 $J_2^{1/2}$ as a function of σ_m at failure for various loading rate for PW, PP and PK sandstones	37

LIST OF FIGURES (Continued)

Figure	Page
5.2 Elastic modulus (E) as a function of the rate of second order stress invariant ($\partial J_2/\partial t$) for PW, PP and PK sandstones	42
5.3 Distortional strain energy density (W_d) as a function of mean stress (σ_m) for PW, PP and PK sandstones	44

LIST OF SYMBOLS AND ABBREVIATIONS

A	=	Empirical constant
c	=	Cohesion
E	=	Elastic modulus
G	=	The shear modulus
$J_2^{1/2}$	=	The second order of stress invariant
K_{Ic}	=	The static fracture toughness
K_{Id}	=	The dynamic fracture toughness
k	=	Loading rates
W_d	=	The distortional strain energy density
W_0	=	The constant
α	=	The constant
β	=	Empirical constant
ε_1	=	Principal strains
ε_2	=	Principal strains
ε_3	=	Principal strains
ϕ	=	Internal friction angle
κ	=	Empirical constant
μ	=	The coefficient of permanent lateral deformation
ν	=	Poisson's ratio
σ_R	=	The constant stress rate

LIST OF SYMBOLS AND ABBREVIATIONS (Continued)

σ_c	=	Compressive strength
σ_m	=	mean stress
σ_1	=	Maximum principal stress
σ_2	=	Intermediate principal stress
σ_3	=	Minimum principal stress
ω	=	shear planes
ξ	=	Empirical constant
$\partial\sigma_1/\partial t$	=	Loading rate

CHAPTER I

INTRODUCTION

1.1 Background and rationale

The effects of loading rate or stress decay (corrosion) on the compressive strength elastic modulus of rocks have long been recognized. It has been found that rock compressive strength deformation modulus decrease with the loading rate (Kumar, 1968; Farmer, 1983; Jaeger and Cook, 1979; Cristescu and Hunsche, 1998). A primary concern of this effect arises when one applies the laboratory-determined properties of intact rock in the design and stability analysis of rock under in-situ conditions. The strength properties obtained from laboratory testing under a relatively high loading rate (normally about 0.5-1.0 MPa per second as specified by the American Society for Testing and Materials – ASTM) tend to be greater than those of the geologic structures during constructions. The discrepancy between the laboratory-determined properties and the actual in-situ properties also depends on rock types, loading characteristics and the project duration. Some obvious examples for such cases include the rock foundation of dams, reservoirs, bridges and buildings. The load rate applied onto the rock foundations during construction process is significantly lower than that obtained from the laboratory test samples. As a result, if the rock is strongly sensitive to the loading rate, the design based on the laboratory-determined properties may not be conservative. To an extreme condition excessive settlement or even failure of the foundations may occur. Even though many

researchers have investigated the loading rate effects on the strengths of various rock types, such effects have never been explicitly incorporated into the strength criteria. In addition, the study on the loading rate effect on the rock strength and elasticity under confined condition has been extremely rare.

1.2 Research objectives

The objectives of this research are to experimentally assess the effect of loading rate on the compressive strength of three types of sandstone and to derive a strength criterion that explicitly incorporates the loading effect. The sandstone specimens belong to the Phra Wihan, Phu Phan, and Phu Kradung formations. These sandstones are commonly found in the north and northeast of Thailand and have impacts on many engineering structures in the region.

1.3 Scope and limitations

1. Laboratory experiments are conducted on specimens from three types of sandstone from Phu Kradung, Pra Wihan, and Phu Phan formations.
2. Laboratory testing is made under various loading rates ranging from 0.001, 0.01, 0.1, 1 to 10 MPa per second with the confining pressures varying from 0, 3, 7 to 12 MPa.
3. All tests are conducted under ambient temperature.
4. Up to 20 samples are tested for each rock type.
5. The minimum and maximum diameters of cylindrical specimens are 1.5 and 2 inches. The size of rectangular blocks is 2x2x4 inches.
6. All tested rocks are prepared in the laboratory.

1.4 Research methodology

As shown in Figure 1.1, the research methodology comprises 6 steps including literature review, sample collection and preparation, laboratory testing (uniaxial compressive strength test, quasi-static test, triaxial test), development of mathematical relations, discussions and conclusions and thesis writing.

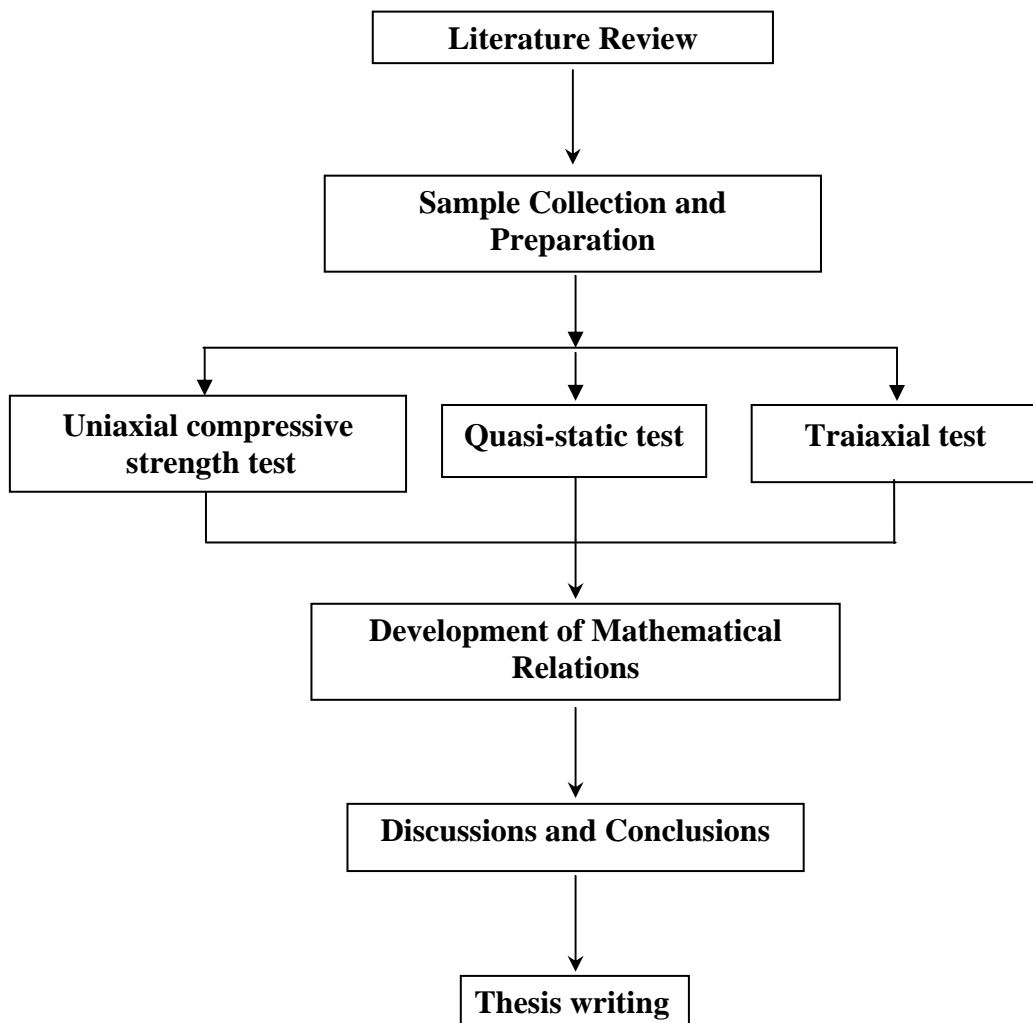


Figure 1.1 Research methodology

1.4.1 Literature review

Literature review is carried out to improve an understanding of loading rate testing of rock under confining pressure knowledge. The sources of information are from journals, technical reports, and conference papers. A summary of the literature review is given in the thesis.

1.4.2 Sample collection and preparation

Sandstone samples are collected from the site. A minimum of 3 sandstone types are collected. Sample preparations are carried out in the laboratory at the Suranaree University of Technology. Specimens prepared for the uniaxial compressive strength test are 54 mm in diameter and 135 mm long. Specimens for the quasi-static test are 37 mm in diameter and 92.5 mm long. Specimens for the triaxial test prepared as 50×50×100 cm rectangular blocks. A minimum of 20 specimens are prepared for each test and each rock types.

1.4.3 Laboratory test

The laboratory testing is divided into three groups; i.e. uniaxial compressive strength test, quasi-static loading test and triaxial Compressive Strength test. The rock strengths and elasticity will be determined in the laboratory under various loading rates ranging from 0.001, 0.01, 0.1, 1 to 10 MPa per second with the confining pressures varying from 0, 3, 7 to 12 MPa. Three samples are tested for each loading rate and confining pressure. The sample preparation, test methods and calculation follow relevant ASTM standard practices, as much as practical. The elastic modulus and compressive strength are measured during the tests.

1.4.3.1 Uniaxial compressive strength tests

The objective of uniaxial compressive strength tests is to determine the ultimate strength and the deformability of the rock specimens under uniaxial compression at various loading rates. The test procedures follow the American Society for Testing and Materials (ASTM D7012-07) and the suggested methods by ISRM (Bieniawski and Bernede., 1978). The test is performed by applying uniform axial stress to the rock cylinder and measuring the increase of axial strains as a function of time. The cylindrical test specimens are drilled, cut, and ground to have a length-to diameter ratio of 2.5 with a diameter of 54 mm. All specimens are loaded by the compression machine model ELE-ARD2000 with capacity of 2000 kN. The specimens are loaded axially to failure under stress rate of 0.01, 0.1, 1 to 10 MPa per second. The post-failure characteristics are observed and recorded.

1.4.3.2 Quasi - static loading tests

The objective of Quasi-static test determines the rock strength as affected by time-dependent behavior. The specimens are loaded axially to failure at constant stress rate of 0.001 MPa per second. The loading rate at 0.001 MPa per second is equivalent to 3.6 MPa per hour. Three samples for rock types are tested for each loading rate.

1.4.3.3 Triaxial compressive strength tests

The objective of the triaxial compression strength tests is to determine the triaxial compressive strength of rock specimens under various loading rates. Triaxial compressive strength tests are performed on three rock specimens under three confining pressures. The confining pressures ($\sigma_2 = \sigma_3$) are 3, 7 and 12

MPa. The experimental procedure follows the American Society for Testing and Materials (ASTM D7012-07) and ISRM suggested method (Bieniawski and Bernede., 1978). The dial gages are installed to measure the axial displacement. Axial load σ_1 is continuously increased. The specimen is loaded until the rock specimen fails. During the test, the axial deformation, and time are monitored. The maximum load at the failure and failure modes are recorded. The axial stress, axial strain, and the failure stress values are calculated.

1.4.4 Development of mathematical relations

The mathematical relationship between the rock mechanical properties and the loading rate are determined. A strength criterion with loading rate parameters is developed from the test results for use to predict the rock strengths and deformations that are subjected to the construction loads under in-situ condition.

1.4.5 Thesis writing and presentation

All research activities, methods, and results are documented and compiled in the thesis.

1.5 Thesis contents

This research thesis is divided into six chapters. The first chapter includes background and rationale, research objectives, scope and limitations and research methodology. **Chapter II** presents results of the literature review to improve an understanding of rock compressive strength as affected by loading rate. **Chapter III** describes sample collection and preparation. **Chapter IV** describes the laboratory testing. **Chapter V** presents development of a strength criterion. **Chapter VI** presents discussions, conclusions and recommendation for future studies.

CHAPTER II

LITERATURE REVIEW

Relevant topics and previous research results are reviewed to improve an understanding of loading rate testing of rock under confining pressures. Results from the review are summarized as follows.

Hashiba et al. (2006) studied the loading-rate dependency for Tago tuff, Sanjome andesite and Akiyoshi marble. The loading-rate dependency of peak strength in these experiments shows a close relation with the creep stress-dependency of creep life. Under confining pressure, the corrected stress–strain curve, obtained by multiplying the stress of the complete stress–strain curve obtained at the fast strain rate by a constant determined by the ratio between the fast strain rate and slow strain rate, is nearly coincident with the stress–strain curve for the slow strain rate. This is an interesting result and represents new knowledge that may help elucidate failure mechanisms in the post-failure region. The loading-rate dependency of stress in the alternating strain rate experiment was most clearly observed when the stress–strain curve becomes flat, parallel to the strain axis.

Okubo et al. (2006) performed uniaxial compression tests and uniaxial tension tests on coal, with particular attention to two concerns. The first was to measure the loading rate dependence of the peak strength of coal. Anthracite samples were subjected to alternating slow and fast strain rates. Measured variations in stress during this process were used to estimate the loading rate dependence of peak strength. The second objective was to obtain complete stress–strain curves for coal under

uniaxial tensile stress. It is difficult to hold samples secure during a tensile test; consequently, such curves have yet to be obtained. This study presents a successful application of the authors' method to the analysis of coal samples, yielding a complete stress–strain curve under tensile stress. The two methods presented here hold promise for application not only to anthracite but also to a wide variety of coals. It is possible to derive the values of the constants used in constitutive equations from the obtained experimental results. The results were obtained in the present study are the complete stress–strain curve for the uniaxial tension test showed ductility, with some residual strength. Comparison of the uniaxial tension strength with the conventional test of indirect tensile strength shows that the latter is 2–3 times higher than the uniaxial tension strength. The peak strength of coal has a relatively low dependence on strain rate under both uniaxial compressive stress and uniaxial tensile stress.

Zhang et al. (1999) studied the fracture toughness of Fangshan gabbro and Fangshan marble and measured over a wide range of loading rates, $k = 10^{-2} - 10^6$ MPa $m^{1/2} s^{-1}$. The testing results indicated that the critical time was generally shorter than the transmitted wave peak time, and the differences between the two times had a weak increasing tendency with loading rates. The experimental results for rock fracture showed that the static fracture toughness K_{Ic} of the rock was nearly a constant, but the dynamic fracture toughness K_{Id} of the rock ($k \geq 10^4$ MPa $m^{1/2} s^{-1}$) increased with the loading rate.

Wang (2008) studied the influence of loading rate on shear band (SB) pattern and entire deformational characteristics and investigated numerically using FLAC. In elastic and strain-softening stages, the constitutive relations are linear. A composite Mohr-Coulomb criterion with tension cut-off is used. For lower and moderate

loading rates, a SB whose inclination angle and thickness are not influenced by loading rate bisects the specimen, so that the post-peak slopes of stress-axial strain curve and stress-lateral strain curve are not related to loading rate. Higher loading rate leads to the conjugate SBs, resulting in less steep post-peak stress-axial strain curve and stress-lateral strain curve. At the same axial strain, higher loading rate leads to shorter SB. With an increase of loading rate, the precursor to failure is more apparent unless the loading rate is very high. At higher loading rate, the great fluctuation in stress exists so that the axial strain corresponding to the peak stress is estimated inappropriately. In strain-softening stage, higher loading rate results in ductile lateral strain-axial strain curve, Poisson's ratio-axial strain curve and volumetric strain-axial strain curve as well as higher peak of volumetric strain and the corresponding axial strain

Backers et al. (2003) studied the influence of loading rate on mechanical properties of rock and the resulting initiation and propagation of fractures. They investigated the influence of loading rate on fracture toughness, fracture roughness and microstructure of sandstone samples subjected to Mode I loading. Fracture toughness is dependent on the fracture velocity. At low velocities, fracture toughness, K_{IC} ; remains almost constant. Exceeding a threshold of fracture velocity, fracture toughness increases significantly. Fracture roughness also increases with increasing loading rate.

Wang (2005) studied the influence of confining pressures from 0 to 28 MPa, which acts on the two lateral edges of rock specimen in plane strain compression, on the shear failure processes and patterns as well as on the macroscopically mechanical responses were numerically modeled by use of FLAC. The numerical results show

that with an increase of confining pressure the peak strength of axial stress-axial strain curve and the corresponding axial strain linearly increase; the residual strength and the stress drop from the peak strength to the residual strength increase; the failure modes of rock transform from the multiple shear bands close to the loading end of the specimen (confining pressure = 0-0.1 MPa), to the conjugate shear bands (0.5-2.0 MPa), and then to the single shear band (4-28 MPa). Once the tip of the band reaches the loading end of the specimen, the direction of the band changes so that the reflection of the band occurs. At higher confining pressure, the new-formed shear band does not intersect the imperfection, bringing extreme difficulties in prediction of the failure of rock structure.

Stavrogin and Tarasov (2001) studied the properties of rocks in the regime where in the deformations are continued beyond the peak strength to collapse which is hence essential for understanding the rupture process. In particular, it is the properties of rocks in the post-failure regime that determine the energy consumption during rupture, the possible loss of stability of the process and its evolution. The tests were all conducted in uniaxial compression. The specimen was subjected to a specific constant strain rate from the onset of load until complete collapse. Similar changes in mechanical behaviour were observed in specimens of marble, granite, ore, sandstones and lignite. Thus both the peak strength and ductility increased with increase in strain rate, the drop modulus M reduced in the post-peak region of the curves, and residual strength increased. Analyzing the results of the above-mentioned investigations and those conducted by other authors, it is clear that under conditions of uniaxial compression, the properties of most rocks change with increase in strain rate according to the classic kinetic concept in strength of materials, i.e., both the strength

of these rocks and the energy required for their rupture increase. The same general trends in property variation were observed under increasing levels of confining pressure, σ_2 . The similarity in effect of increased strain rate and confining pressure on rock properties described above was established by a detailed comparative study of the effect of each of these parameters. The results of these studies are outlined below. The relationships between the residual (irreversible) axial $\Delta\varepsilon_1$ and lateral $\Delta\varepsilon_2$ strains, plotted from processing the results of the curves given in Figure 2.1 (a) are presented in Figure 2.1 (b). The tangent of the angle of inclination of these relationships, in the selected coordinate system, is equal to the coefficient of permanent lateral deformation μ . Increase in the strain rate led to a reduction in the value of μ , as in tests conducted under confining pressure. Irreversible changes in the volumetric strain were also the same for both testing methods. In terms of the discussed above statistical model, a reduction in μ and increase in permanent volumetric strains in the pre-failure and post-failure strength regimes indicate the participation of a large number of structural elements and shear planes ω in the deformation process, which should be accompanied by an increased degree of disintegration in the material. Thus the disintegration of specimens when loaded under (i) static confined pressures and (ii) a high rate of loading was almost the same, and 1.5 times more than the disintegration under static uniaxial compression. It is known that the degree of crushability of a material increases with increase in strain rate. The objective was to study the effect of variation in test conditions (confining pressure and strain rate) introduced at different stages of loading, on the development of deformation processes. Curve 1 in Figure 2.2 (a) was obtained by testing a specimen under uniaxial compression until complete failure at a static strain rate ($\dot{\varepsilon}_1 = 2 \times 10^{-1} \text{ s}^{-1}$); curve 2 was obtained under dynamic

loading ($\varepsilon_2 = 2 \times 10^{-1} \text{ s}^{-1}$). Curves 3, 4 and 5 correspond to tests conducted under varying conditions. Points A in the diagrams correspond to the beginning of a sharp rise in strain rate from $\varepsilon = 2 \times 10^{-6} \text{ s}^{-1}$ to $\varepsilon = 2 \times 10^{-1} \text{ s}^{-1}$ at different stages of post-peak deformation. Curve 1 in Figure 2.2 (b) was obtained by quasi-static uniaxial loading. Curve 2 indicates the data obtained by testing at the same rate but at a confining pressure $\sigma_2 = 4 \text{ MPa}$. Curves 3, 4 and 5 were obtained under conditions of variable loading. The curves in Figure 2.2 (a) and (b) are very similar. Application of confining pressure and increase in strain rate produced similar effects throughout the post-peak deformation regime, i.e., hardening of material, increase in plasticity and reduction in drop modulus M . The results of experiments in which the test conditions were reversed are shown in Figure 2.2 (c) and (d). Up to point A in Figure 2.2 (c) the specimen was subjected to dynamic loading at a strain rate of $\varepsilon_1 = 2 \times 10^{-1} \text{ s}^{-1}$, while in Figure 2.2 (d) the load was applied under a confining pressure $\sigma_2 = 4 \text{ MPa}$. Beyond points A, in the first case the strain rate was reduced suddenly to the quasi-static level ($\varepsilon_1 = 2 \times 10^{-6} \text{ s}^{-1}$); in the second case, the confining pressure was dropped to atmospheric (i.e., no confining pressure).

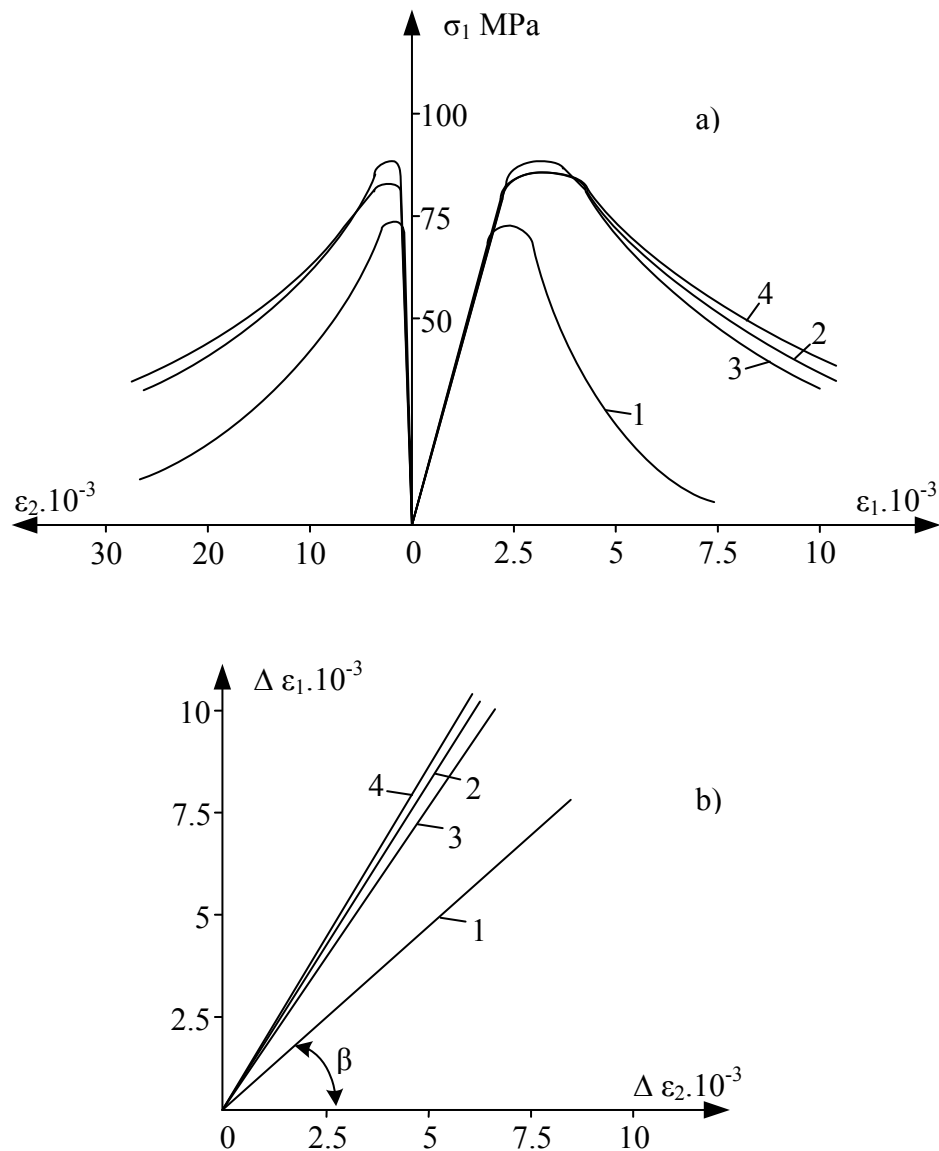


Figure 2.1 Relationships between (a) $\sigma_1 - \varepsilon_1 - \varepsilon_2$ and (b) $\Delta \varepsilon_1 - \Delta \varepsilon_2$ for marble under the following test conditions: 1—uniaxial compression at a strain rate $\varepsilon_1 = 2 \times 10^{-6} \text{ s}^{-1}$; 2—uniaxial compression at a strain rate $\varepsilon_1 = 2 \times 10^{-1} \text{ s}^{-1}$; 3, 4—compression with confining pressure $\sigma_2 = 4 \text{ MPa}$ and strain rate $\varepsilon_1 = 2 \times 10^{-6} \text{ s}^{-1}$ (Stavrogina and Tarasov, 2001).

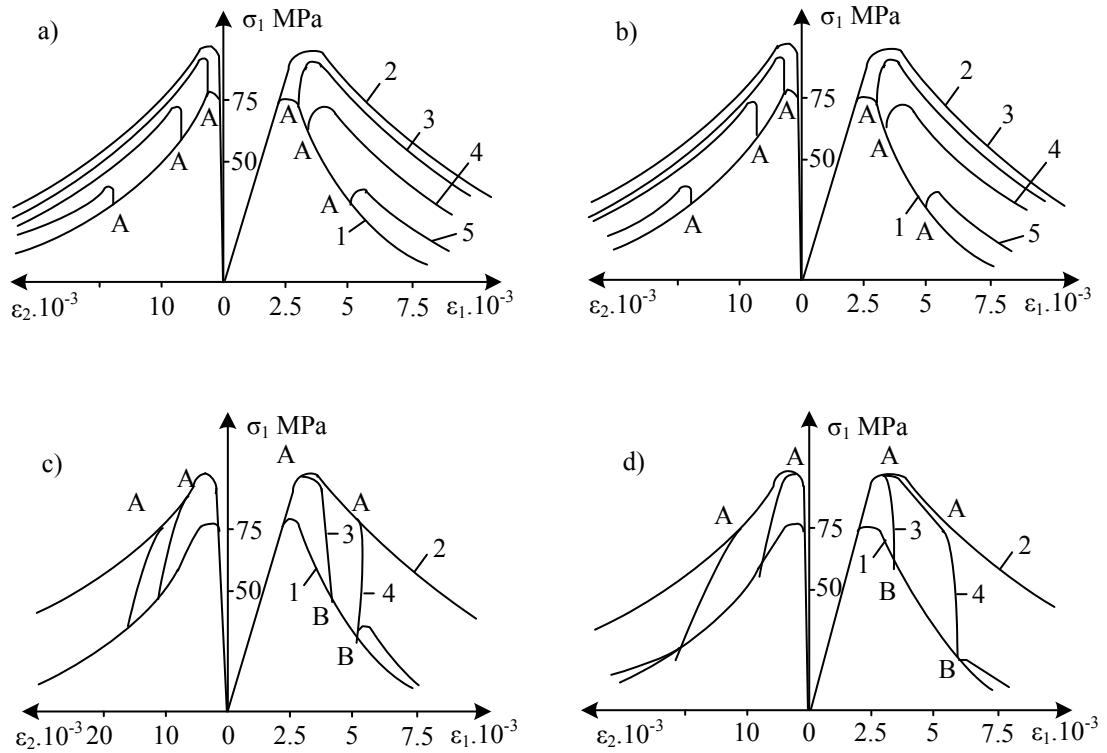


Figure 2.2 Stress-strain relationships ($\sigma_1 - \epsilon_1 - \epsilon_2$) obtained by testing marble under the following conditions. (a) 1—strain rate $\epsilon_1 = 2 \times 10^{-6} \text{ s}^{-1}$; 2—strain rate $\epsilon_1 = 2 \times 10^{-1} \text{ s}^{-1}$; 3, 4, 5—strain rate $\epsilon_1 = 2 \times 10^{-6} \text{ s}^{-1}$ up to point A; $\epsilon_1 = 2 \times 10^{-1} \text{ s}^{-1}$ beyond A. (b) 1—strain rate $\epsilon_1 = 2 \times 10^{-6} \text{ s}^{-1}$; 2—strain rate $\epsilon_1 = 2 \times 10^{-6} \text{ s}^{-1}$; 3, 4, 5—changing confinement regime (strain rate $\epsilon_1 = 2 \times 10^{-6} \text{ s}^{-1}$ beyond A), (c) 1—strain rate $\epsilon_1 = 2 \times 10^{-6} \text{ s}^{-1}$; 2—strain rate $\epsilon_1 = 2 \times 10^{-1} \text{ s}^{-1}$; 3, 4—strain rate $\epsilon_1 = 2 \times 10^{-1} \text{ s}^{-1}$ up to point A; strain rate $\epsilon_1 = 2 \times 10^{-6} \text{ s}^{-1}$ beyond A. (d) 1—strain rate $\epsilon_1 = 2 \times 10^{-6} \text{ s}^{-1}$; 2—strain rate $\epsilon_1 = 2 \times 10^{-6} \text{ s}^{-1}$; 3, 4—confining pressure $\sigma_2 = 4 \text{ MPa}$ to point A; confining pressure reduced to atmospheric (i.e., uniaxial compression) beyond A—at strain rate $\epsilon_1 = 2 \times 10^{-6} \text{ s}^{-1}$ (Stavrogin and Tarasov, 2001).

CHAPTER III

SAMPLE PREPARATION

3.1 Introduction

The tested sandstones are from three sources: Phra Wihan, Phu Phan and Phu Kradung sandstones (hereafter designated as PW, PP and PK sandstones) (Figure 3.1). These rocks are classified as fine-grained quartz sandstones with highly uniform texture and density. These brittle rocks are medium strong. Their mechanical properties play a significant role in the stability of tunnels, slope embankments and dam foundations in the north and northeast of Thailand.

3.2 Sample preparation and collection

Sample preparation is conducted in laboratory facility at the Suranaree University of Technology. The specimens are core, cut and ground to obtain the perpendicularity and parallelism that comply with the ASTM (D 4543-85) specifications (Figures 3.2 through 3.3). Specimens prepared for the uniaxial compressive strength test have 54 mm in diameter and 135 mm long (Figure 3.4). Specimens for the quasi-static test have 37 mm in diameter and 92.5 mm long (Figure 3.5). Specimens for the triaxial test are prepared as 50×50×100 mm rectangular blocks (Figure 3.6). A minimum of 20 specimens are prepared for each test and each rock type. They are oven-dried before testing.

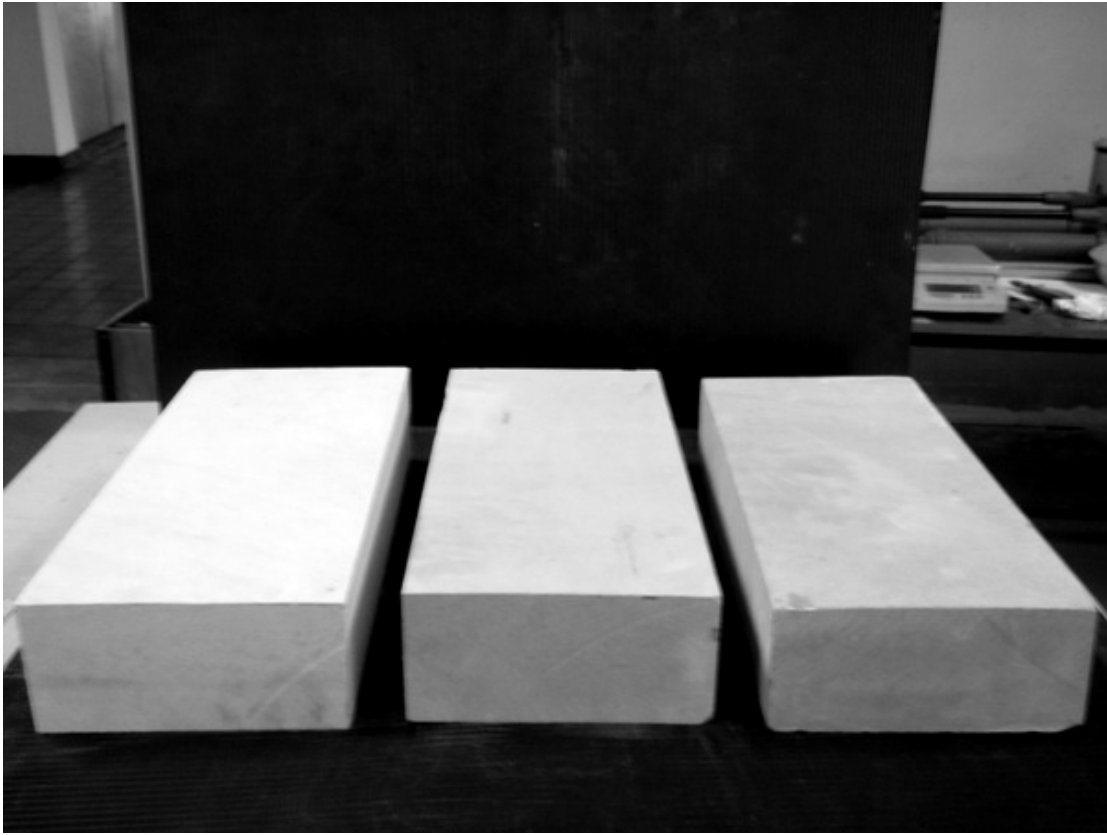


Figure 3.1 PW, PP and PK sandstones blocks with nominal size of 10 cm x 20 cm x 40 cm are collected from Saraburi province.



Figure 3.2 Laboratory core drilling of PK sandstone. The core drilling machines (model SBEL 1150) are used to drill core specimens using diamond impregnated bit with diameters of 54 mm and 37 mm.



Figure 3.3 A core specimen of PK sandstone is cut by a cutting machine.



Figure 3.4 PK, PP and PW sandstones specimens prepared for the uniaxial compressive strength test have 54 mm in diameter and with L/D ratio of 2.5

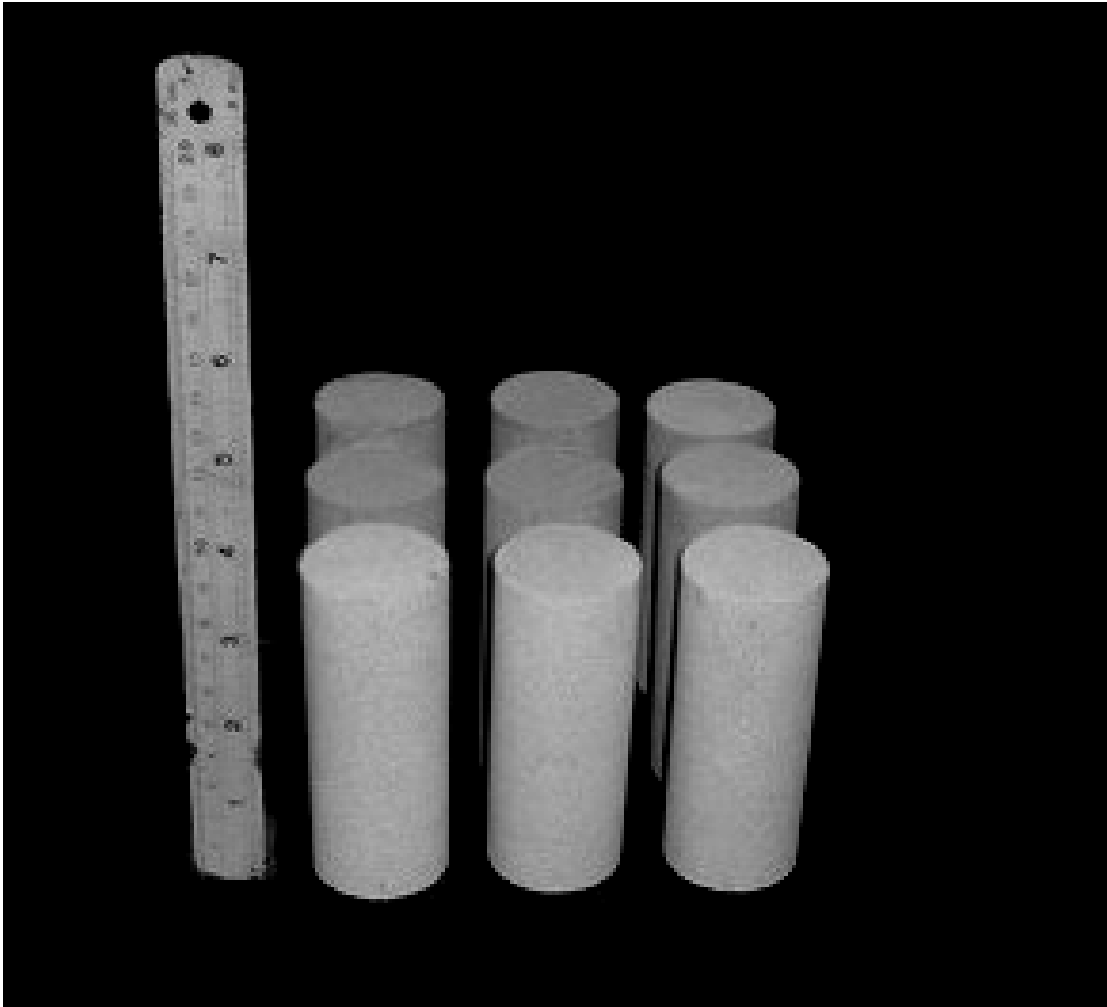


Figure 3.5 PW, PP and PK sandstones specimens for the quasi-static test have 37 mm in diameter with L/D ratio of 2.5

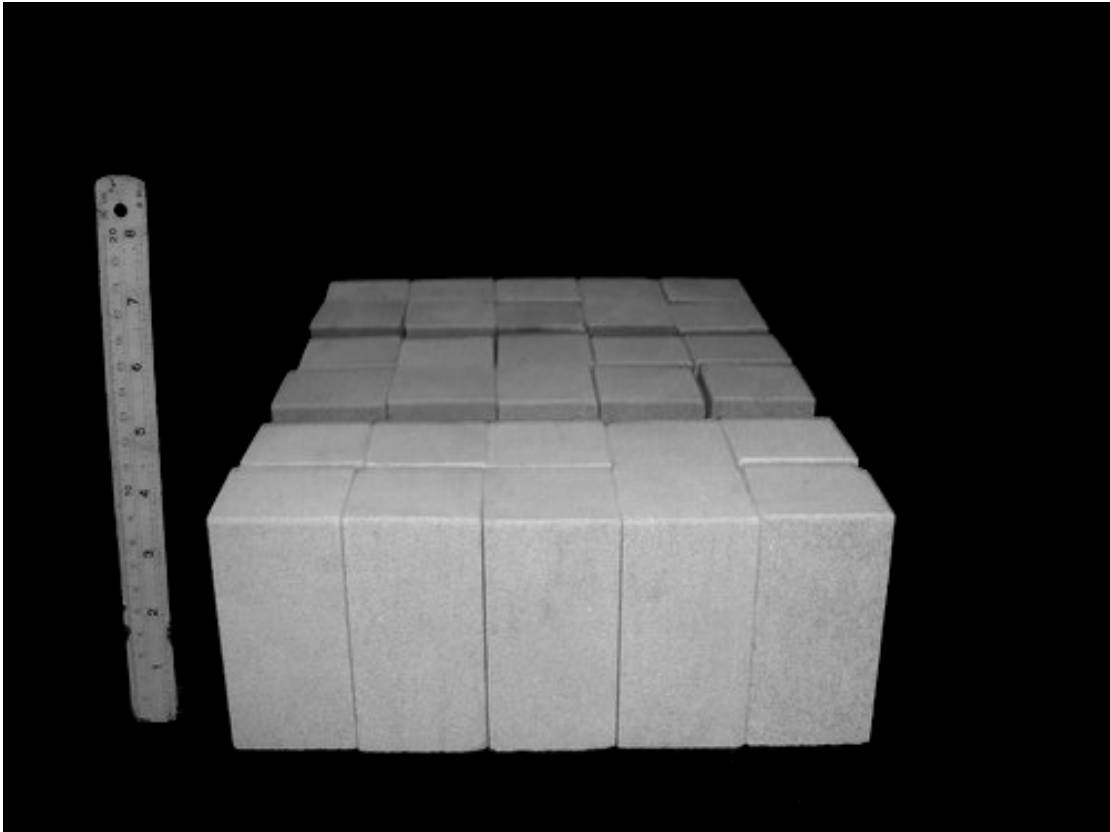


Figure 3.6 The rectangular block specimens of PW, PP and PK sandstones used in the polyaxial testing are cut and ground to have a nominal dimension of $50 \times 50 \times 100 \text{ cm}^3$.

CHAPTER IV

LABORATORY EXPERIMENTS

4.1 Introduction

The objective of the laboratory experiments is to assess the effects of loading rates on the compressive strength and elasticity of the sandstone specimens. This chapter describes the method and results of the laboratory experiments. The tests are divided into three groups; i.e. rate-controlled uniaxial compressive strength tests, quasi-static loading tests and rate-controlled triaxial compressive strength tests.

4.2 Rate-controlled uniaxial compressive strength tests

The objective of the rate-controlled uniaxial compressive strength tests is to determine the ultimate strength and the deformability of the rock specimens under uniaxial compression at various loading rates. The test procedures follow the American Society for Testing and Materials (ASTM D 7012-07) and the suggested methods by ISRM (Bieniawski and Bernede., 1978). The tests are performed by applying uniform axial stress under constant rate to the rock cylinder and measuring the increase of axial strains as a function of time (Figure 4.1). The specimens are loaded axially to failure under stress rates varying from 0.01, 0.1, 1 to 10 MPa per second. The post-failure characteristics are observed and recorded.

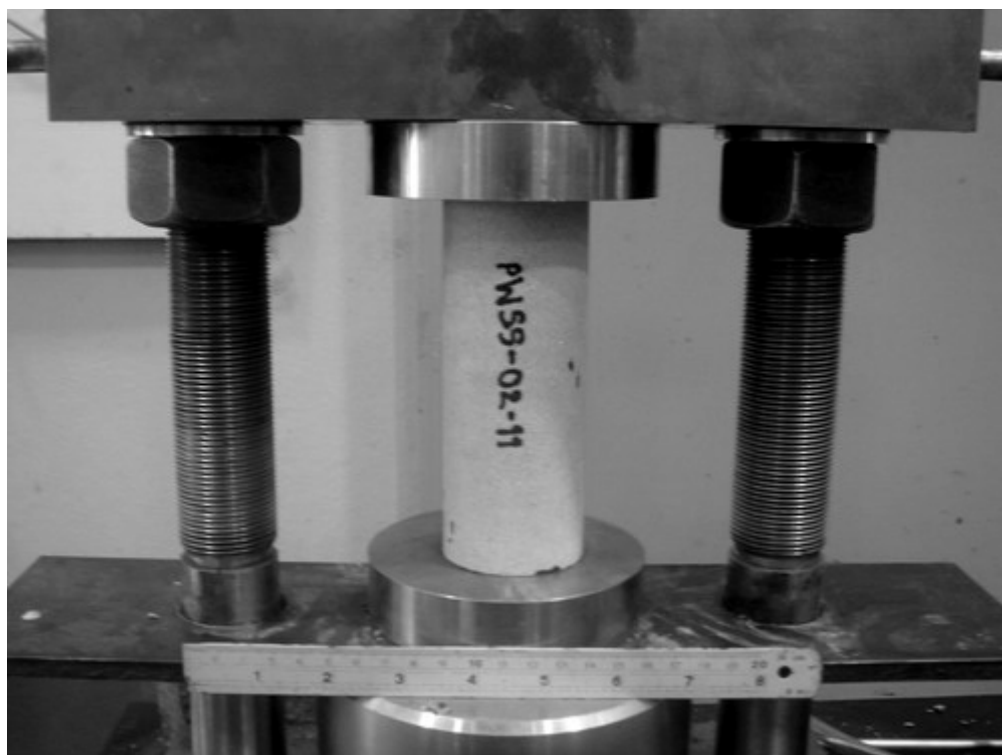


Figure 4.1 A cylindrical specimen for PW sandstone is tested under rate-controlled uniaxial compression.

4.3 Quasi - static loading tests

The objective of the quasi-static test is to determine the sandstone strength as affected by very low loading rate. The tests are performed by applying uniform axial stress to the rock cylinder and measuring the increase of axial strains as a function of time (Figure 4.2). The constant axial stress is progressively increased for each hour to obtain an average loading rate of 0.001 MPa per second. The loading rate at 0.001 MPa per second is equivalent to 3.6 MPa per hour.

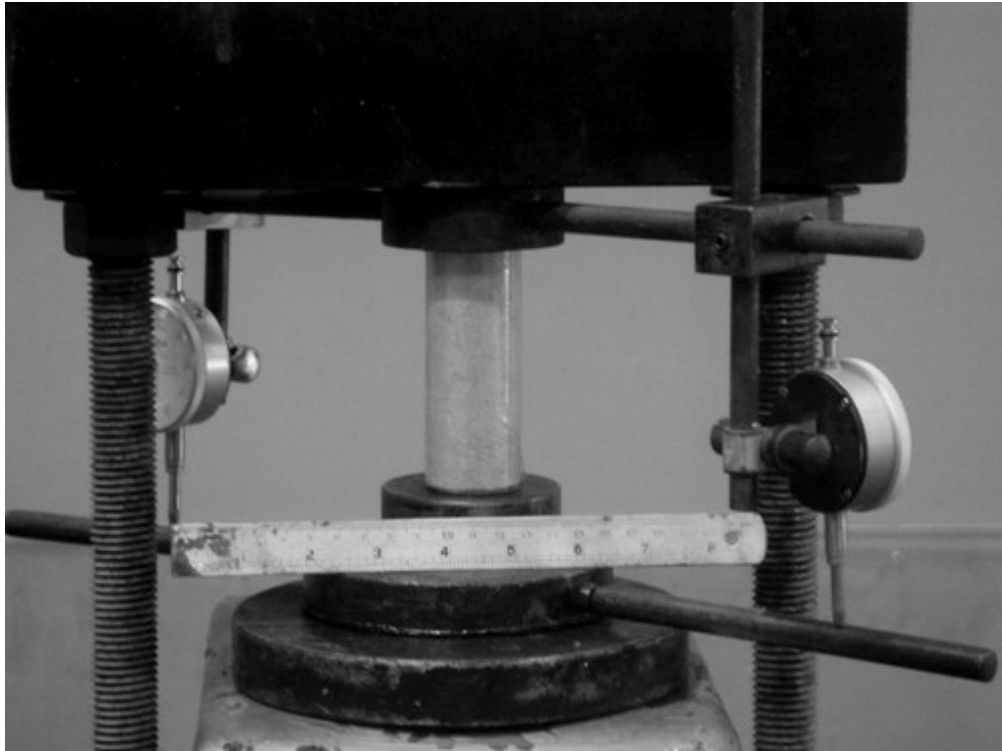


Figure 4.2 A cylindrical specimen for PK sandstone is tested under quasi-static loading.

4.4 Rate-controlled triaxial compressive strength tests

The objective of the rate-controlled triaxial compressive strength test is to determine the effects of loading rate on the compressive strength of the three sandstones under various confining pressures. The confining pressures range from 3, 7 to 12 MPa, and the constant axial stress rates from 0.001, 0.01, 0.1, 1.0 to 10 MPa/s. The specimen deformations monitored in the three principal directions are used to calculate the principal strains during loading. The failure stresses are recorded and mode of failure examined.

The polyaxial load frame has been used in this study because the cantilever beams with pre-calibrated dead weight can apply a truly constant lateral stress (confining pressure) to the specimen. Figure 4.3 shows the polyaxial load frame used.

These lateral confining mechanism and deformation measurements are isolated from the axial loading system. Such arrangement is necessary particularly for the triaxial testing under very high loading rates. For example at the loading rate of 10 MPa/s the sandstone specimens can fail within 5-8 seconds. The induced specimen dilation is too rapid for Hoek cell or triaxial cell to release the pressurized oil and maintain a constant confining pressure during loading. The excess oil pressure due to rapid dilation could lead to an error of the strength results.

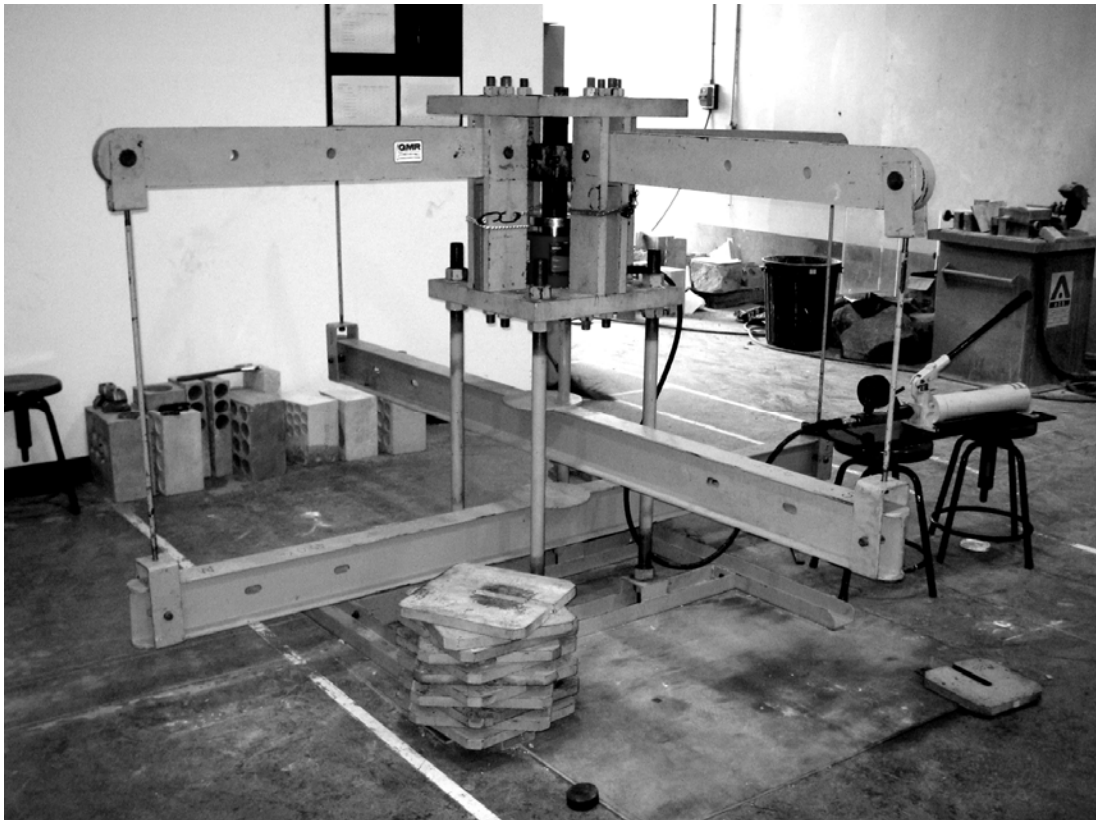


Figure 4.3 A polyaxial load frame used for the rate-controlled triaxial compressive strength tests.

4.5 Test results

Table 4.1 through Table 4.3 summarizes the test results on PW, PP and PK sandstones. Figure 4.4 plots the axial stress-strain curves obtained from the uniaxial and quasi-static loading tests under various loading rates for the three sandstones. Despite the intrinsic variability among the specimens the curves tend to show loading-rate dependent behavior of the rocks. The higher the loading rates applied, the higher the rock strength and stiffness obtained. Figures 4.5 through 4.7 give the triaxial compression test results for the loading rates ($\partial\sigma_1/\partial t$) of 0.01, 0.1, and 1.0 MPa/s for the three sandstones. The tangent elastic moduli at 50% failure stress have been calculated from the measured stress-strain curves obtained from all uniaxial and triaxial loading specimens. The elastic moduli are plotted as a function of $\partial\sigma_1/\partial t$ in Figure 4.8. For all sandstones tested here the elastic modulus exponentially decreases with the applied $\partial\sigma_1/\partial t$, which can be best represented by a power equation: $E = \kappa (\partial\sigma_1/\partial t)^\xi$, where κ and ξ are empirical constants. Figure 4.8 gives numerical values for these constants. The average Poisson's ratios are 0.36, 0.38 and 0.15 for the PP, PW and PK sandstones, respectively. They tend to be independent of the loading rates. Post-test observations indicate that under confining pressures of 7 MPa or less, the specimens fail by a combination of compressive shear and splitting tension modes. Under the confining pressure of 12 MPa extension fractures dominate.

The maximum principal stresses at failure are plotted as a function of the minimum principal stresses (confining pressures) in Figure 4.9. Based on the Coulomb strength criterion the cohesion (c) and internal friction angle (ϕ) of the rocks have been calculated and presented in the figure. The loading-rate effect apparently acts at all

Table 4.1 Summary of test results of Phra Wihan sandstone.

Confining pressure (MPa)	Loading Rate (MPa/s)	Compressive Strength, σ_c (MPa)	Elastic Modulus, E (GPa)
0	10	83.50	N/A
	1	68.60	12.5
	0.1	64.62	10.8
	0.01	57.80	11.1
	0.001	46.80	6.3
3	10	110	N/A
	1	102	10.25
	0.1	85.50	8.20
	0.01	80.16	6.40
	0.001	73.64	7.69
7	10	130	N/A
	1	121.67	10.97
	0.1	109.26	9.39
	0.01	95.48	8.85
	0.001	90.6	7.67
12	10	145	N/A
	1	146.62	12.09
	0.1	143.94	11.89
	0.01	135.04	11.54
	0.001	130.20	10.39

magnitudes of the confining pressures. The failure envelopes clearly show that the failure stresses decrease with decreasing loading rates. The effect of the confining pressures on the loading-rate dependency of the tested sandstones remains inconclusive due to the relatively narrow range of the applied confining pressures and the intrinsic variations of the rocks.

Table 4.2 Summary of test results of Phu Phan sandstone.

Confining pressure (MPa)	Loading Rate (MPa/s)	Compressive Strength, σ_c (MPa)	Elastic Modulus, E (GPa)
0	10	92.72	N/A
	1	85	13.34
	0.1	80.7	13.67
	0.01	76.1	13.17
	0.001	68.40	10.3
3	10	121	N/A
	1	108.61	10.43
	0.1	98.86	9.62
	0.01	93.50	9.23
	0.001	87.40	7.72
7	10	153.10	N/A
	1	147.40	10.71
	0.1	133.80	10.42
	0.01	125	8.62
	0.001	109.66	7.59
12	10	166.70	N/A
	1	154.10	11.73
	0.1	162.88	12.54
	0.01	162.10	12.58
	0.001	153.14	10.11

Table 4.3 Summary of results of Phu Kradung sandstone.

Confining pressure (MPa)	Loading Rate (MPa/s)	Compressive Strength, σ_c (MPa)	Elastic Modulus, E (GPa)
0	10	80.20	N/A
	1	71.30	9.10
	0.1	61.00	8.40
	0.01	60.00	8.39
	0.001	46.80	7.90
3	10	117.34	N/A
	1	97.40	8.89
	0.1	91.95	8.19
	0.01	80.43	7.00
	0.001	78.65	5.36
7	10	143.90	N/A
	1	131.90	10.31
	0.1	123.60	9.59
	0.01	109.66	8.92
	0.001	99.25	6.74
12	10	161.65	N/A
	1	150.38	10.98
	0.1	134.10	8.24
	0.01	120.20	9.66
	0.001	117.00	8.98

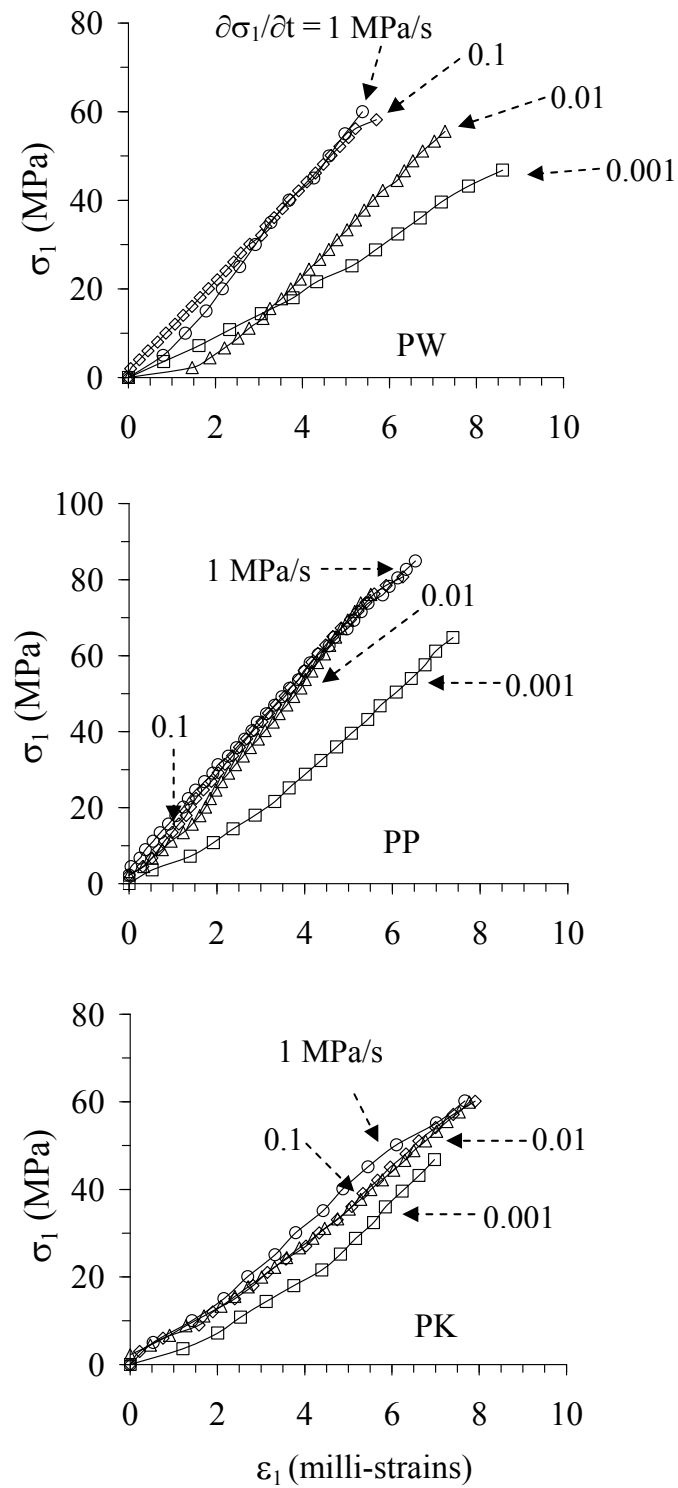


Figure 4.4 Uniaxial compressive strength and quasi-static testing result under loading rates varied from 0.001, 0.01, 0.1 and 1.0 MPa/s, for PW, PP and PK sandstones.

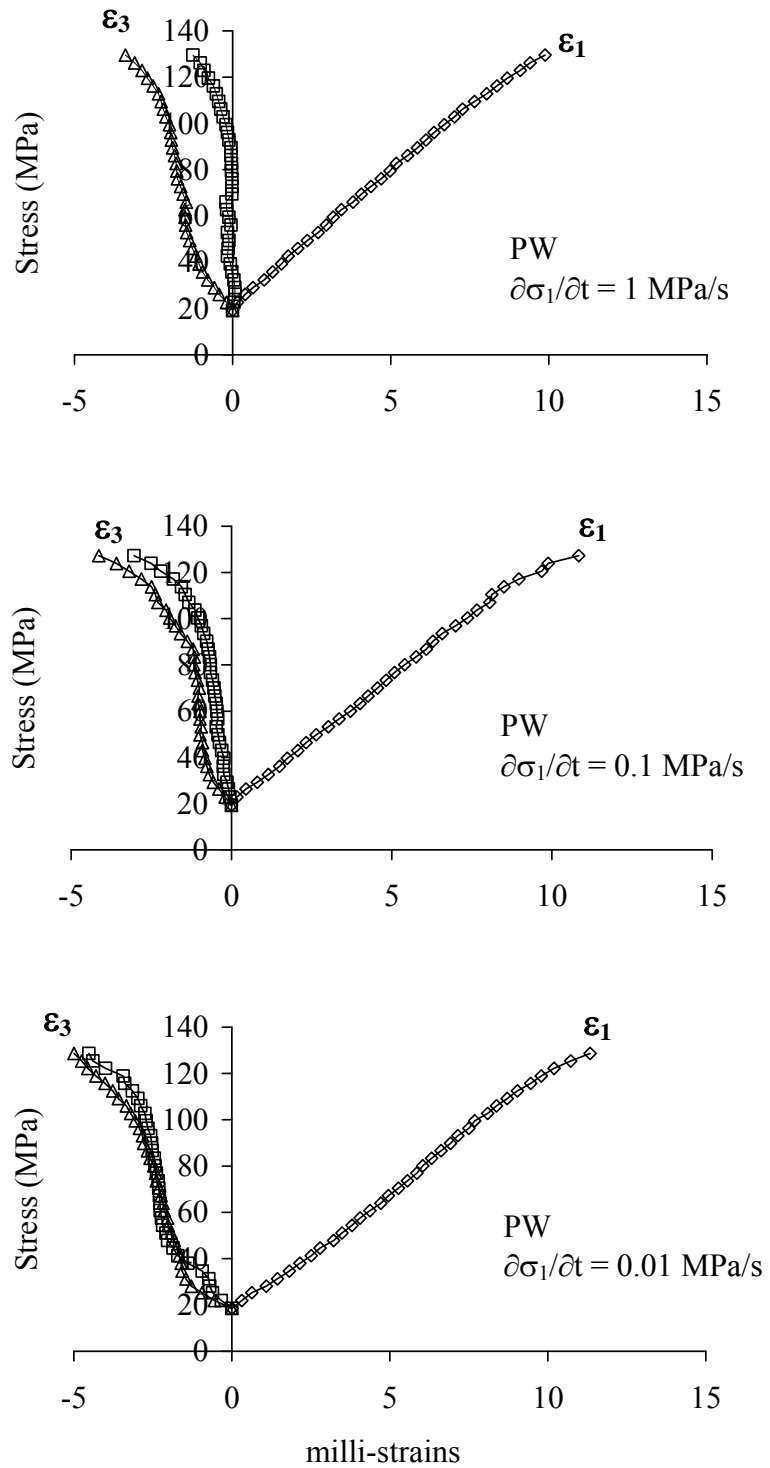


Figure 4.5 Examples of triaxial compressive strength testing results for PW sandstone with axial loading rates of 1, 0.1, and 0.01 MPa/s (from top to bottom).

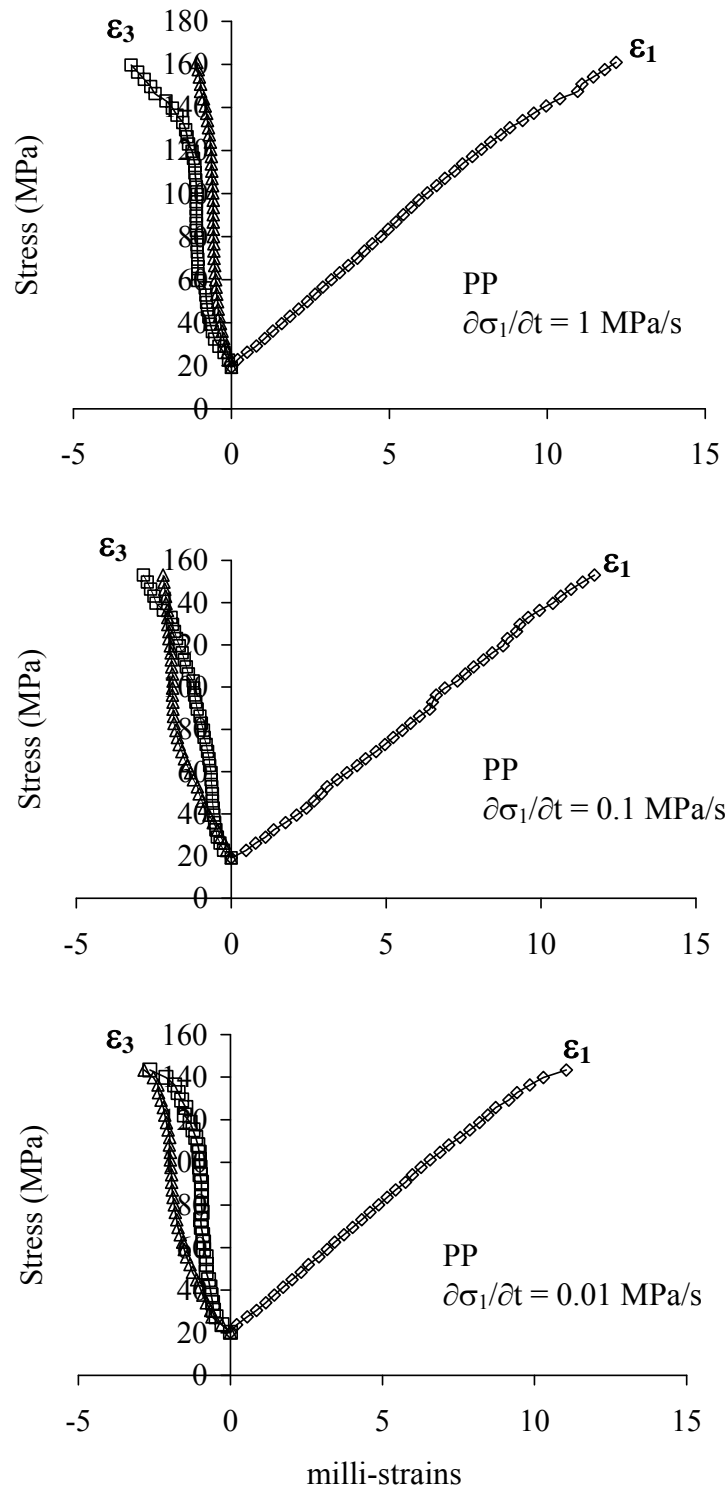


Figure 4.6 Examples of triaxial compressive strength testing results for PP sandstone with axial loading rates of 1, 0.1, and 0.01 MPa/s (from top to bottom).

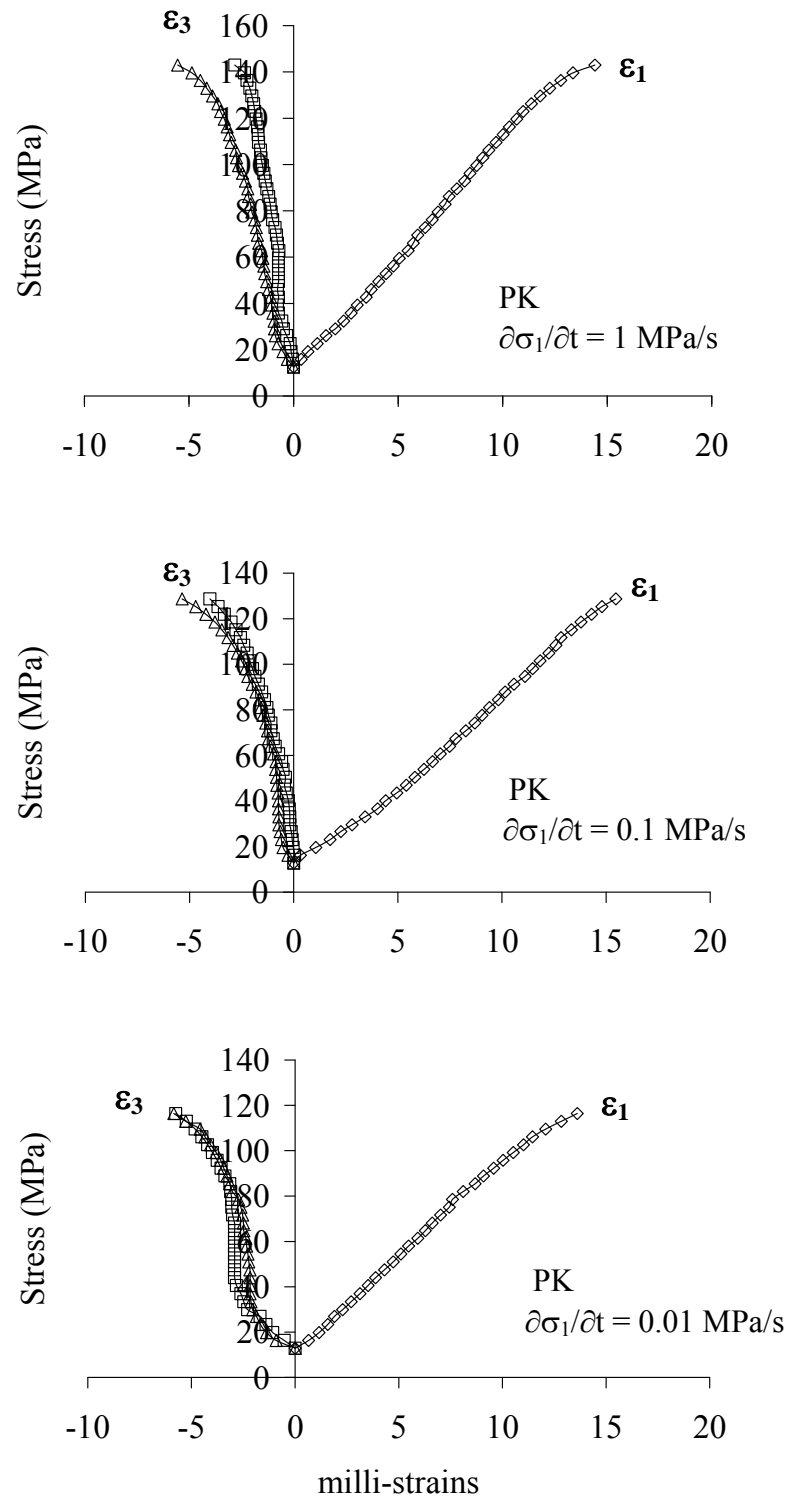


Figure 4.7 Examples of triaxial compressive strength testing results for PK sandstone with axial loading rates of 1, 0.1, and 0.01 MPa/s (from top to bottom).

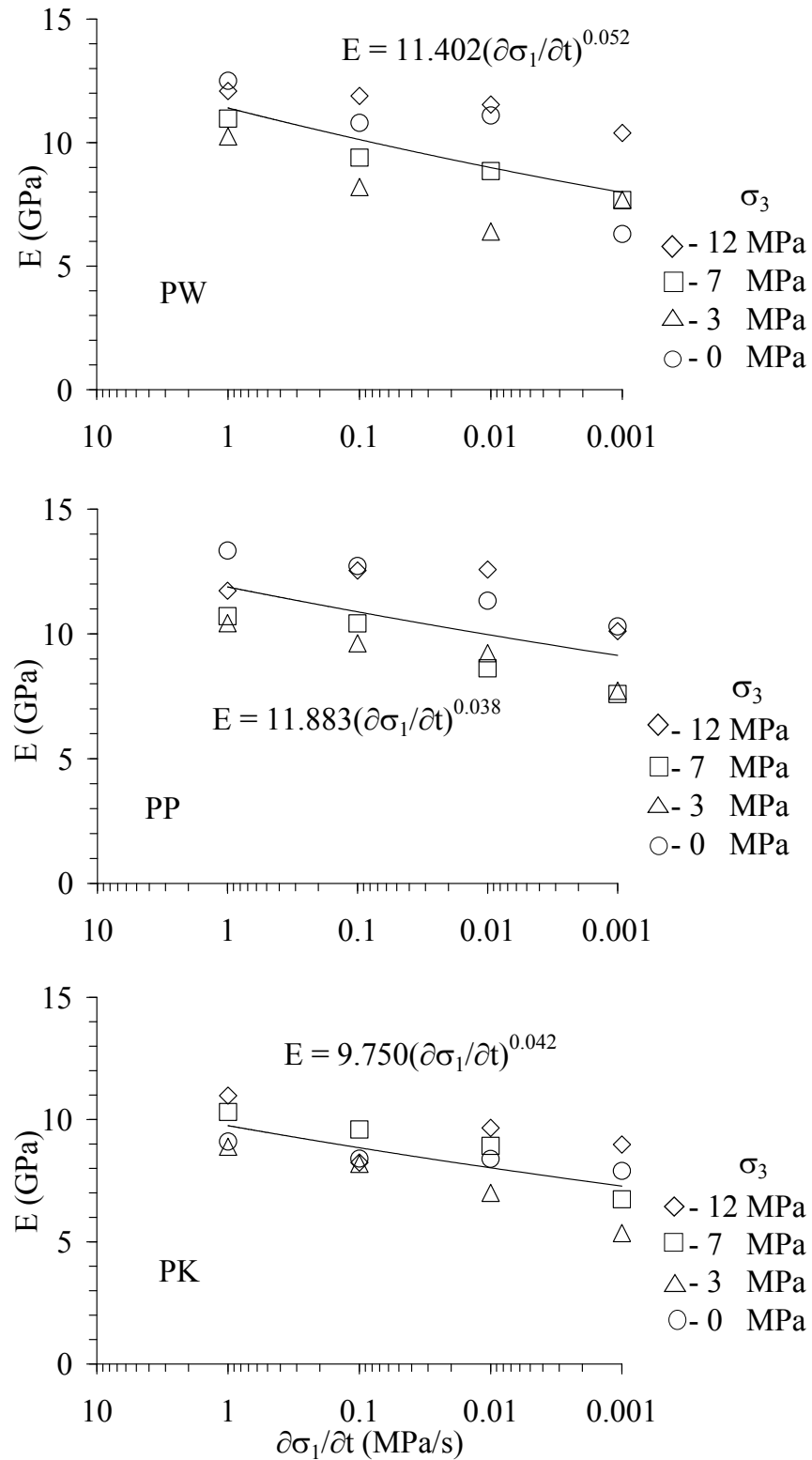
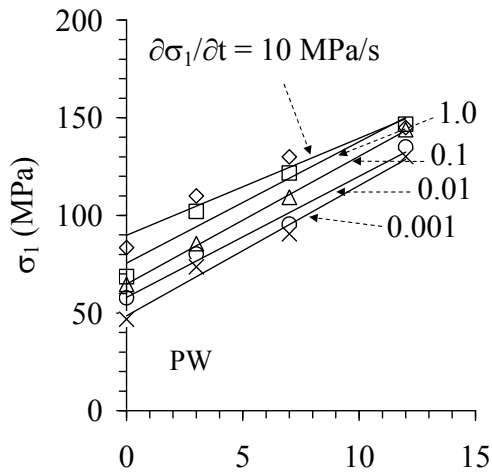
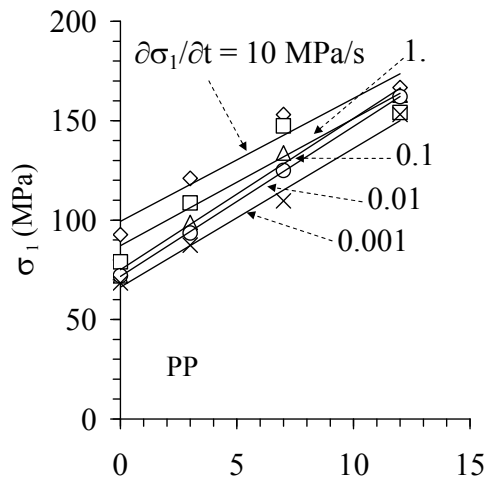


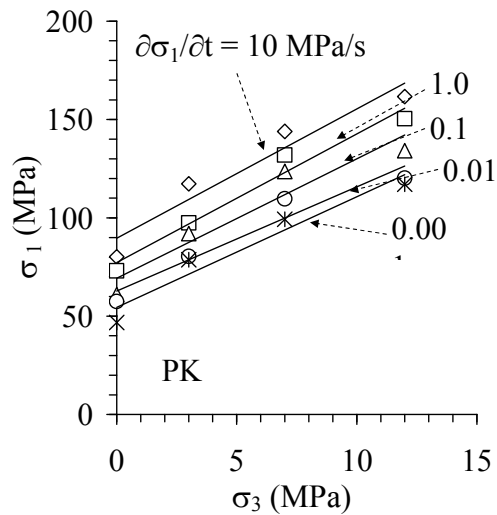
Figure 4.8 Elastic modulus (E) as a function of applied loading rate ($\partial\sigma_1/\partial t$) for PW, PP and PK sandstones.



$\partial\sigma_1/\partial t$ (MPa/s)	c (MPa)	ϕ (degree)
10	20	42
1.0	15	46
0.1	13	47
0.01	13	43
0.001	9	48



$\partial\sigma_1/\partial t$ (MPa/s)	c (MPa)	ϕ (degree)
10	20	46
1.0	17	47
0.1	14	50
0.01	13	50
0.001	13	49



$\partial\sigma_1/\partial t$ (MPa/s)	c (MPa)	ϕ (degree)
10	14	53
1.0	15	47
0.1	14	46
0.01	14	43
0.001	12	44

Figure 4.9 Maximum principal stress (σ_1) as a function of minimum principal stress (σ_3) at failure various loading rates for PW, PP and PK sandstones.

CHAPTER V

DEVELOPMENT OF A STRENGTH CRITERION

5.1 Introduction

The failure envelopes presented in Chapter IV show the maximum principal stresses (σ_1) as a function of the minimum principal stresses (σ_3) which are not directly applicable for a stability analysis of geological structures. This is because the changes with time of the in-situ rock stresses during constructions or excavations may occur in all three principal directions. It is therefore necessary to develop a multi-axial strength criterion that can incorporate the effect of loading rate for the three principal directions.

5.2 Multi-axial strength criterion for triaxial testing

To examine the three-dimensional stresses at failure as affected by the loading rate, the second order of the stress invariants ($J_2^{1/2}$) at failure are calculated and presented as a function of the mean stress (σ_m) as shown in Figure 5.1 and Tables 5.1 through 5.3.

$$J_2^{1/2} = (1/6)[\sigma_1^2 - 2\sigma_1\sigma_3 + \sigma_3^2] \quad (5.1)$$

$$\sigma_m = (1/3)(\sigma_1 + 2\sigma_3) \quad (5.2)$$

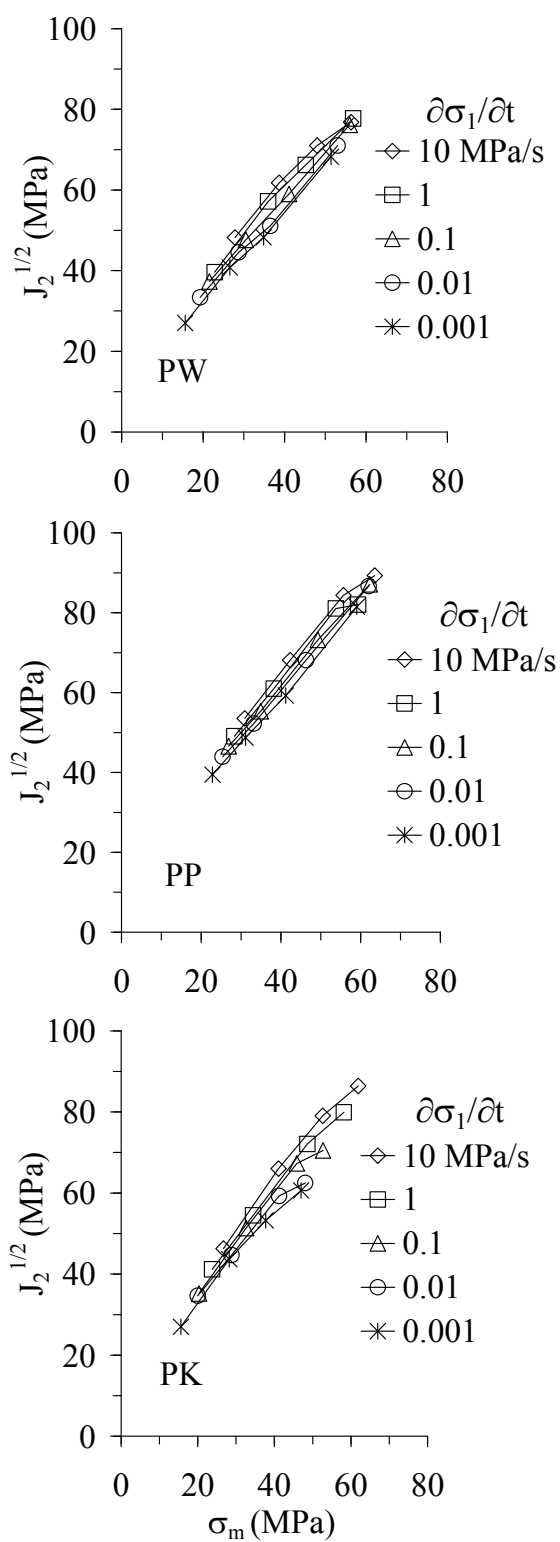


Figure 5.1 $J_2^{1/2}$ as a function of σ_m at failure for various loading rate for PW, PP and PK sandstones.

Table 5.1 Test results of Phra Wihan sandstone.

Loading Rate (MPa/s)	σ_3 (MPa)	σ_2 (MPa)	σ_1 (MPa)	$J_2^{1/2}$ (MPa)	σ_m (MPa)
10	0.00	0.00	83.5	48.21	27.83
	3.00	3.00	110	61.78	38.67
	7.00	7.00	130	71.01	48.00
	12.00	12.00	145	76.79	56.33
1	0.00	0.00	68.6	39.61	22.87
	3.00	3.00	102	57.16	36.00
	7.00	7.00	121.67	66.20	45.22
	12.00	12.00	146.62	77.72	56.87
0.1	0.00	0.00	64.62	37.31	21.54
	3.00	3.00	85.5	47.63	30.50
	7.00	7.00	109.26	59.04	41.09
	12.00	12.00	143.94	76.18	55.98
0.01	0.00	0.00	57.8	33.37	19.27
	3.00	3.00	80.16	44.55	28.72
	7.00	7.00	95.48	51.08	36.49
	12.00	12.00	135.04	71.04	53.01
0.001	0.00	0.00	46.80	27.02	15.60
	3.00	3.00	73.64	40.78	26.55
	7.00	7.00	90.6	48.27	34.87
	12.00	12.00	130.2	68.24	51.40

where $J_2^{1/2}$ is stress invariants for triaxial testing, σ_m is mean stress for triaxial testing,

σ_1 is maximum principal stress and σ_3 is minimum principal stress.

The failure envelopes in the $J_2^{1/2}$ - σ_m diagram still show the effect of the loading rate. At the same σ_m a higher loading rate yields a greater $J_2^{1/2}$ value. This implies that the rate-dependent stiffness should also be considered in the derivation of a strength criterion.

Table 5.2 Test results of Phu Phan sandstone.

Loading Rate (MPa/s)	σ_3 (MPa)	σ_2 (MPa)	σ_1 (MPa)	$J_2^{1/2}$ (MPa)	σ_m (MPa)
10	0.00	0.00	92.72	53.53	30.91
	3.00	3.00	121.00	68.13	42.33
	7.00	7.00	153.10	84.35	55.70
	12.00	12.00	166.70	89.32	63.57
1	0.00	0.00	85.00	49.07	28.33
	3.00	3.00	108.61	60.97	38.20
	7.00	7.00	147.40	81.06	53.80
	12.00	12.00	154.10	82.04	59.37
0.1	0.00	0.00	80.70	46.59	26.90
	3.00	3.00	98.86	55.34	34.95
	7.00	7.00	133.80	73.21	49.27
	12.00	12.00	162.88	87.11	62.29
0.01	0.00	0.00	76.10	43.94	25.37
	3.00	3.00	93.50	52.25	33.17
	7.00	7.00	125.00	68.13	46.33
	12.00	12.00	162.10	86.66	62.03
0.001	0.00	0.00	68.40	39.49	22.80
	3.00	3.00	87.40	48.73	31.13
	7.00	7.00	109.66	59.27	41.22
	12.00	12.00	153.14	81.49	59.05

5.3 A rate-dependent strength criterion

The rate of stress invariant $\partial J_2/\partial t$ can be derived as a function of the principal stress σ_1 and σ_3 . The stress rate along σ_1 is denoted as σ_R .

$$\partial J_2/\partial t = (\partial/\partial t) (1/6) [(\sigma_1 - \sigma_2)^2 + (\sigma_2 - \sigma_3)^2 + (\sigma_3 - \sigma_1)^2] \quad (5.3)$$

For the uniaxial and triaxial stress conditions where the confining pressures ($\sigma_2 = \sigma_3$) are constant with time and the axial stress is increased at a constant rate ($\sigma_1 = \sigma_R t$), equation (5.3) can be simplified as:

Table 5.3 Test results of Phu Kradung sandstone.

Loading Rate (MPa/s)	σ_3 (MPa)	σ_2 (MPa)	σ_1 (MPa)	$J_2^{1/2}$ (MPa)	σ_m (MPa)
10	0.00	0.00	80.20	46.30	26.73
	3.00	3.00	117.34	66.01	41.11
	7.00	7.00	143.90	79.04	52.63
	12.00	12.00	161.65	86.40	61.88
1	0.00	0.00	71.30	41.17	23.77
	3.00	3.00	97.40	54.50	34.47
	7.00	7.00	131.90	72.11	48.63
	12.00	12.00	150.38	79.89	58.13
0.1	0.00	0.00	61.00	35.22	20.33
	3.00	3.00	91.95	51.36	32.65
	7.00	7.00	123.60	67.32	45.87
	12.00	12.00	134.10	70.49	52.70
0.01	0.00	0.00	60.00	34.64	20.00
	3.00	3.00	80.43	44.70	28.81
	7.00	7.00	109.66	59.27	41.22
	12.00	12.00	120.20	62.47	48.07
0.001	0.00	0.00	46.80	27.02	15.60
	3.00	3.00	78.65	43.68	28.22
	7.00	7.00	99.25	53.26	37.75
	12.00	12.00	117.00	60.62	47.00

$$\partial J_2 / \partial t = (2/3) \sigma_R (\sigma_1 - \sigma_3) \quad (5.4)$$

where σ_R is the constant stress rate along the major principal direction (in MPa/s).

An empirical relation is first proposed to represent the rock elastic modulus as affected by the stress rates along the principal directions. Assuming that the rocks are linearly elastic and isotropic the elastic modulus (E) is defined as:

$$E = A (\partial J_2 / \partial t)^\beta \quad (5.5)$$

where A and β are empirical constants.

Figure 5.2 presents the rock elastic modulus (E) as a function of $\partial J_2/\partial t$ for all confining pressures, and lists the numerical values of the constants A and β for the three sandstones. The rock elasticity decreases exponentially with decreasing $\partial J_2/\partial t$. The exponent β indicates the slope of the curve on the semi-log scale while the constant A represents the rock elastic modulus at the stress invariant rate of $1.0 \text{ MPa}^2/\text{s}$.

5.4 Strength criterion based on strain energy density

To incorporate the loading-rate dependency of the rock strength and stiffness, the distortional strain energy density (W_d) is proposed to describe the rock stresses at failure, where W_d can be expressed as (Jaeger and Cook, 1979):

$$W_d = J_2/(2G) \quad (5.6)$$

$$G = E/(2(1 + \nu)) \quad (5.7)$$

where G is the rock shear modulus which can be defined as a function of the loading rates along the principal directions by substituting equation (5.5) into equation (5.7), and assuming that the rock Poisson's ratio is independent of the loading rates. Equation (5.6) implies that W_d at failure for each rock type is constant under a given confining pressure. This means that as the loading rate decreases, the shear modulus G and the second order of the stress invariant J_2 at failure decrease with the same proportion.

The effect of loading rate is assumed to act equally at all magnitudes of the mean stress (σ_m). A strength criterion that implicitly incorporates the loading rate effect can therefore be presented as:

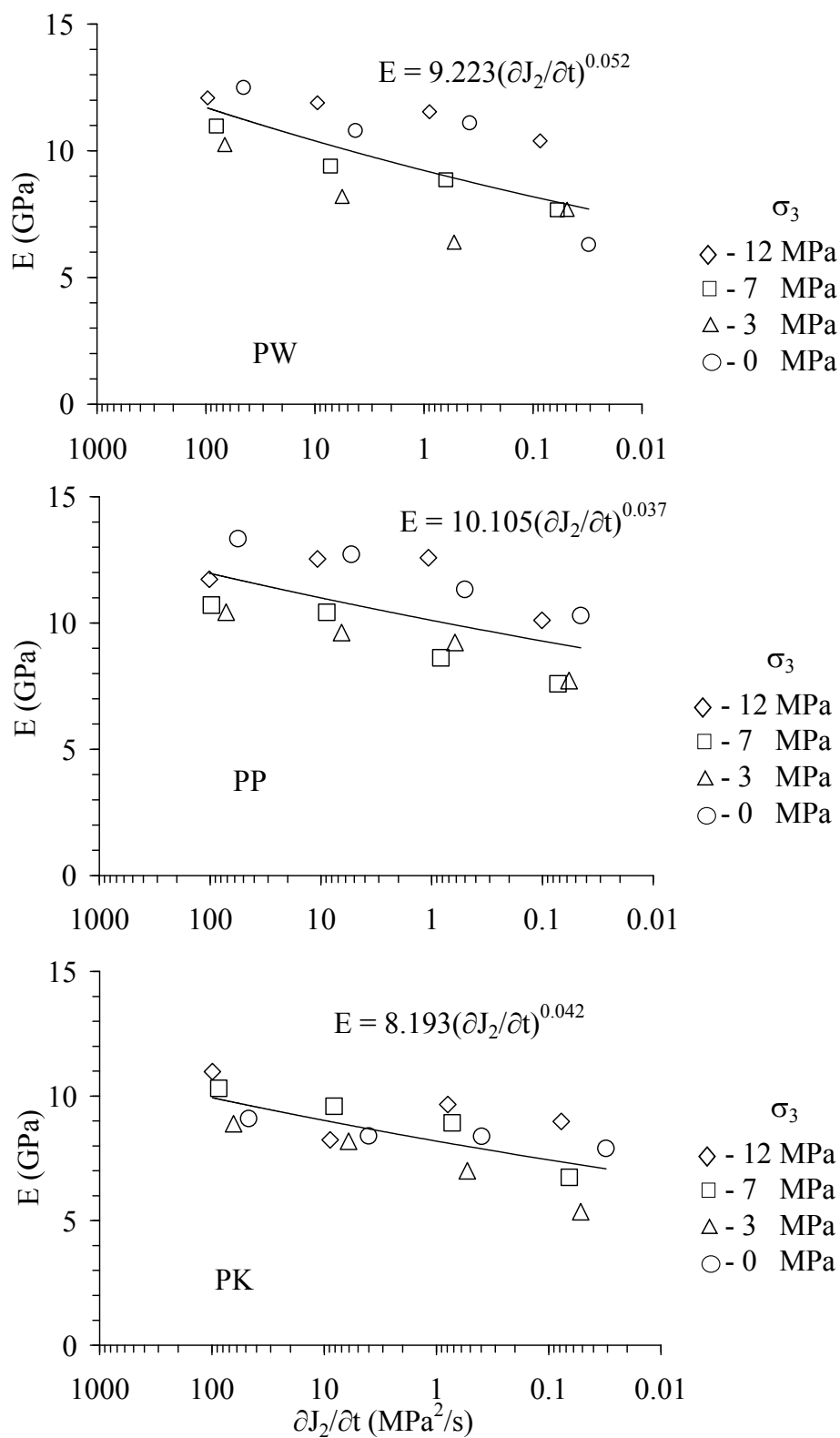


Figure 5.2 Elastic modulus (E) as a function of the rate of second order stress invariant ($\partial J_2 / \partial t$) for PW, PP and PK sandstones.

$$W_d = \alpha \sigma_m - W_0 \quad (5.8)$$

The constants α and W_0 depend on rock type, where α represents the slope of the failure envelope and W_0 is the intercept.

From equations (5.3) through (5.7) W_d for the three sandstones can be calculated from the uniaxial and triaxial test results and is presented as a function of σ_m in Figure 5.3. Regression analysis of the test data provides the numerical values for the constants α and W_0 , as given in the figure. Very good correlation coefficients (greater than 0.90) are obtained.

Here the loading rate effect on the rock elasticity has been incorporated into the proposed strength criterion by using equation (5.5). The loading rate effect on the failure stresses is considered by deriving the strength criterion in the form of the distortional strain energy density [equation (5.8)]. The proposed strength criterion is based on an assumption that under a given mean stress, the same distortional strain energy density is required to fail the specimen for each rock type. As a result a single failure envelope can represent the rock strengths under various loading rates and mean stresses.

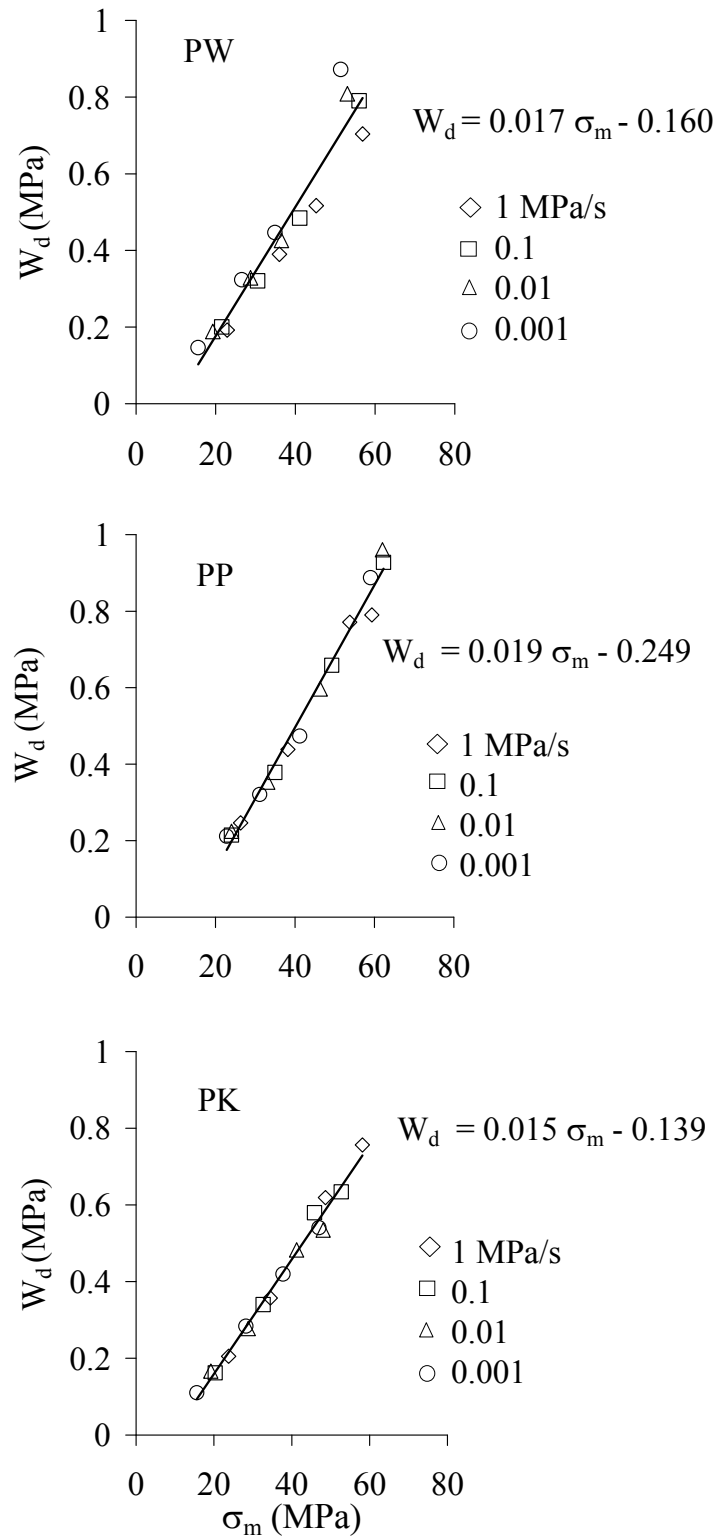


Figure 5.3 Distortional strain energy density (W_d) as a function of mean stress (σ_m)

for PW, PP and PK sandstones.

CHAPTER VI

DISCUSSIONS, CONCLUSIONS, AND RECOMMENDATIONS FOR FUTURE STUDIES

6.1 Discussions and conclusions

The proposed strength criterion, equation (5.8), can be applied to assess the stability conditions of any in-situ rock subjected to stress rates along the three principal directions. This can be accomplished by first performing uniaxial compressive strength tests of the rock under various loading rates. Assuming that the loading-rate effects act equally under all confining pressures, the elastic modulus can be defined as a function of $\partial J_2/\partial t$, i.e. by determining the empirical constants A and β in equation (5.5). A failure envelope ($W_d - \sigma_m$ curve) can be constructed from the strength test data by using equations (5.6) through (5.8). Note that for other rocks the $W_d - \sigma_m$ failure envelope may not be linear. For soft rocks under high confining pressures a non-linear relation may be used to fit the experimental results in the $W_d - \sigma_m$ diagram. The W_d induced by the loading rates on the three principal stresses under an in-situ condition, probably predicted from numerical simulations, can then be compared against the criterion developed above. If the loading rates of the in-situ rocks are known for all three principal stresses, equation (5.3) should be used to determine $\partial J_2/\partial t$, and subsequently obtaining the elastic modulus as affected by the multi-axial loading rates.

It is concluded from this study that to assess the loading-rate dependency of dry and brittle rocks the strength criterion can be defined in terms of the distortional strain energy density (W_d) as a function of the mean stress (σ_m) at failure. Here the proposed criterion can well describe the uniaxial and triaxial compressive strengths of the PP, PW and PK sandstones for the range of the loading rates from 0.001 to 10 MPa/s with the confining pressures up to 12 MPa. The criterion is based on an assumption that the loading rate effects act equally at all confining pressures. This results in a single failure envelope which is useful for predicting the strength of in-situ rocks subject to loading rates that are different from those used in the laboratory. The proposed strength criterion is applicable for the multi-axial stress rates induced simultaneously along the three principal directions of linearly elastic and isotropic rocks.

6.2 Recommendations for future studies

The uncertainties and adequacies of the research investigation and results discussed above lead to the recommendations for further studies, as follows. The coupled effect of pore pressure should be investigated. Lower loading rates of less than 0.001 MPa/s are desirable. More testing is required on a variety of brittle rocks. More investigation is also desirable to confirm on verity that the effect of loading rate acts equally under all confining pressure. This also suggests that test results under higher confining pressure should be obtained.

REFERENCES

- ASTM D 4543-85. Standard practice for preparing rock core specimens and determining dimensional and shape tolerances. **Annual Book of ASTM Standards**. 04.08. American Society for Testing and Materials: Philadelphia.
- ASTM D 7012-07. Compressive strength and elastic moduli of intact rock core specimens under varying states of stress and temperatures. **Annual Book of ASTM Standards**. 04.08. West Conshohocken: American Society for Testing and Materials: Philadelphia.
- Aubertin, M., Li, L., and Simon, R. (2000). A multiaxial stress criterion for short- and long-term strength of isotropic rock media. **International Journal of Rock Mechanics and Mining Sciences**. 37: 1169-1193
- Backers, T., Fardinb, N., Dresena, G., and Stephanssona, O. (2003). Effect of loading rate on Mode I fracture toughness, roughness and micromechanics of sandstone. **International Journal of Rock Mechanics and Mining Sciences**. 40: 425–433.
- Bieniawski, Z.T. and Bernede, M.J. (1978). Suggested Methods for determining the uniaxial compressive strength and deformability of rock materials. **International Journal of Rock Mechanics and Mining Sciences and Geomechanics Abstracts**. (pp. 135-140). International Society for Rock Mechanics Commission on Standardization of Laboratory and Field Tests.
- Blanton, T.L. (1981). Effect of strain rates from $10^{-2}/s$ to $10^1/s$ in triaxial compression tests on three rocks. **International Journal of Rock Mechanics and Mining Sciences and Geomechanics Abstracts**. 18: 47-62.

- Chong, K.P., Harking, J.S., Kuruppu, M.D., and Leskinen, A.I. (1987). Strain rate dependent mechanical properties of western oil shale. In **Proceedings of the 28th US. Rock mechanics Symposium**, Rotterdam: Balkema. pp. 157-164.
- Costin, L.S. (1987). **Time-dependent deformation and failure, Fracture Mechanics of Rock**. Barry Kean Atkinson, Editor. London: Academic Press. 167–215.
- Cristescu, N.D. and Hunsche, U. (1998). **Time Effects in Rock Mechanics**. New York: John Wiley and Sons.
- Daemen, J.J.K., (2009). On the importance, and difficulty, of dealing with the time dependency of engineered structures in, on, or with hard rock. In **Proceedings of the Second Thailand Symposium on Rock mechanics**, Nakhon Ratchasima: Suranaree University of Technology. 2: pp 3-34.
- Farmer, I.W., (1983) **Engineering Behaviour of Rock**, second edition. London: Chapman and Hall.
- Hashiba, K., Okubo, S., and Fukui, K. (2006). A new testing method for investigating the loading rate dependency of peak and residual rock strength. **International Journal of Rock Mechanics and Mining Sciences**. 43: 894-904.
- Ishizuka., Y., Koyama, H., and Komura, S. (1993). Effect of strain rate on strength and frequency dependence of fatigue failure of rocks. **Assessment and Prevention of Failure Phenomena in rock Engineering**. 321-327.
- Jaeger, J.C. and Cook, N.G.W. (1979). **Fundamentals of Rock Mechanics**. London: Chapman and Hall.
- Kohmura, Y. and Inada, Y. (2006). The effect of the loading rate on stress-strain characteristics of tuff. **Journal of the Society of Materials Science**. 55(3): 323-328.

- Kumar, A. (1968). The effect of stress rate and temperature on the strength of basalt and granite. **Geophysics**. 33(3): 501-510.
- Li, Y. and Xia, C. (2000). Time-dependent tests on intact rocks in uniaxial compression. **International Journal of Rock Mechanics and Mining Sciences**. 37: 467-475.
- Okubo, S., Fukui, K., and Qingxin, Q. (2006). Uniaxial compression and tension tests of anthracite and loading rate dependence of peak strength. **International Journal of Coal Geology**. 68: 196-204.
- Okubo, S., Fukui, K., and Jiang, X. (2001). **Loading rate dependency of Young's modulus of rock. Shigen-to-Sozai**. 117(1): 29-35.
- Okubo, S., Nishimatsu, Y., He, C., and Chu, S.Y. (1992). Loading rate dependency of uniaxial compressive strength of rock under water-saturated condition. **Journal of the Society of Materials Science**. 41(463): 403-409.
- Ray, S.K., Sarkar, M., and Singh, T.N. (1999). Effect of cyclic loading and strain rate on the mechanical behaviour of sandstone. **International Journal of Rock Mechanics and Mining Sciences**. 36: 543-549.
- Stavrogin, A.N. and Tarasov, B.G. (2001). **Experimental Physics and Rock Mechanics**. Lisse: A.A. Balkema.
- Vogler, U.W. and Kovari, K. (1978). Suggested methods for determining the strength of rock materials in triaxial compression. **International Journal of Rock Mechanics and Mining Sciences and Geomechanics Abstracts**. 15 (2): 47-54.
- Walsri, C., Poonprakon, P., Thosuwan, R., and Fuenkajorn, K. (2009). Compressive and tensile strengths of sandstones under true triaxial stresses. In **Proceedings**

of the Second Thailand Symposium on Rock mechanics, Nakhon Ratchasima:
Suranaree University of Technology. 2: pp 199-218.

Wang, X.B. (2008). Effect of loading rate on entire deformational characteristics of rock specimen. **Rock and Soil Mechanics**. 29(2): 353-358.

Wang, X.B. (2005). Effect of confining pressure on deformation and failure of rock at higher strain rate. **Journal of Coal Science and Engineering**. 11: 32-36.

Zhang, Z.X., Kou, S.Q., Yu, J., Yu, Y., Jiang, L.G., and Lindqvist, P.A. (1999). Effects of loading rate on rock fracture. **International Journal of Rock Mechanics and Mining Sciences**. 36: 597- 611.

APPENDIX A

TECHNICAL PUBLICATION

TECHNICAL PUBLICATION

Kenkhunthod, N., and Fuenkajorn, K., 2009. **Loading rate effects on strength and stiffness of sandstones under confinement.** In Proceeding 2nd Thailand Symposium on Rock Mechanics. Chonburi, Thailand. 12 - 13 March 2009.

Loading rate effects on strength and stiffness of sandstones under confinement

N. Kenkhunthod & K. Fuenkajorn

Geomechanics Research Unit, Suranaree University of Technology, Thailand

Keyword: Loading rate, compressive strength, elasticity, strain energy, sandstone

ABSTRACTS: Uniaxial and triaxial compressive strength tests have been performed to assess the loading rate effects on the strength and stiffness of sandstone specimens. The applied axial stresses are controlled at constant rates of 0.001, 0.01, 0.1, 1.0 and 10 MPa/s. The confining pressures are varied from 0, 3, 7 to 12 MPa. The sandstone strengths and elastic moduli tend to increase exponentially with the loading rates. The effects seem to be independent of the confining pressures. To consider all three principal stresses at failure the rock stiffness is defined as a function of the rate of the second order of stress invariant ($\partial J_2/\partial t$). Assuming that the energy required to fail the specimen for each rock type is independent of the applied loading rate, a multi-axial strength criterion based on the strain energy density is developed by taking into consideration the rate-dependent strength and stiffness of the rock. The distortional strain energy density (W_d) defined as a function of mean stress (J_1) can well describe the sandstone strengths within the range of the loading rates tested here. The proposed strength criterion is useful for predicting the strength and deformation characteristics of in-situ rocks subject to loading rates that are different from those used in the laboratory.

1 INTRODUCTION

The effects of loading rate on the compressive strength and stiffness of intact rocks have long been recognized (Kumar, 1968; Farmer, 1983; Jaeger & Cook, 1979; Cristescu & Hunsche, 1998). A primary concern of the rate-dependent effect arises when one applies the laboratory-determined properties of intact rock to the design and stability analysis of rock under in-situ conditions. The strength and elastic properties obtained from laboratory testing under a relatively high loading rate (normally about 0.5-1.0 MPa per second, e.g. ASTM D 7012) tend to be greater than those of in-situ rocks during excavations or constructions (e.g. dam foundations and underground openings), which may lead to a non-conservative analysis and design of the relevant geologic structures. Ishizuka (1993), Okubo et al. (1992, 2006) and Kohmura & Inada (2006) conclude from their experimental results that rock uniaxial compressive strengths tend to increase with loading rates and induced strain rates. For brittle rocks the loading rate effects on the elastic modulus remain inconclusive (Blanton, 1981; Chong et al., 1987; Ray et al., 1999; Wang, 2008; Okubo et al., 2001). The mechanisms governing the loading-rate dependency for brittle rocks have been related to the time-

dependent initiation and propagation of the micro-cracks and fractures in the rock matrix (Costin, 1987; Zhang et al., 1999; Ray et al., 1999; Li and Xia, 2000; Aubertin et al., 2000). Extensive review of the time- and rate-dependent issues on the strengths and deformations of hard rocks has been given by Daemen (2009).

Even though numerous studies have been performed to investigate the loading rate effects on the strengths of various rock types, such effects have rarely been incorporated into a strength criteria for practical use. Study on the loading rate effect on the rock strength and elasticity under confined conditions has also been rare.

The objectives of this research are to experimentally assess the effects of loading rate on the compressive strength and stiffness of three sandstones and to derive a strength criterion that can take loading rate effect into consideration. The stress-rate controlled uniaxial and triaxial tests have been performed under various loading rates using a polyaxial load frame. An empirical relationship is derived between the loading rates and the elastic moduli of these brittle rocks. The distortional strain energy density at failure is proposed to describe the sandstone compressive strengths as a function of mean stress.

2 ROCK SAMPLES

Phra Wihan, Phu Phan and Phu Kradung sandstones (hereafter designated as PW, PP and PK sandstones) have been prepared to obtain rectangular block specimens with a nominal dimension of 50×50×100 mm. These rocks are classified as fine-grained quartz sandstones with highly uniform texture and density. These brittle rocks are medium strong. Their mechanical properties play a significant role in the stability of tunnels, slope embankments and dam foundations in the north and northeast of Thailand. The specimens are cut and ground to obtain the perpendicularity and parallelism that comply with the ASTM (D 4543) specifications. Though having different shape the specimens used here have volume and length-to-diameter ratio comparable to those used in the conventional uniaxial and triaxial compression test methods. A minimum of 15 specimens are prepared for each sandstone type. They are oven-dried before testing.

3 UNIAXIAL AND TRIAXIAL COMPRESSION TESTING

A polyaxial load frame equipped with a cantilever beam system (Walsri et al., 2009) has been used to applied constant and uniform lateral stresses (confining pressures) while the axial stress is increased at a constant rate until failure occurs. The confining pressures range from 0, 3, 7 to 12 MPa, and the constant axial stress rates from 0.001, 0.01, 0.1, 1.0 to 10 MPa/s. Neoprene sheets are used to minimize the friction at the interfaces between loading platens and rock surfaces. The specimen deformations monitored in the three principal directions are used to calculate the principal strains during loading. The failure stresses are recorded and mode of failure examined.

The polyaxial load frame has been used in this study because the cantilever beams with pre-calibrated dead weight can apply a truly constant lateral stress to the specimen. These lateral confining mechanism and deformation measurements are isolated from the axial loading system. Such arrangement is necessary particularly for the triaxial testing under very high loading rates. For example at the loading rate of 10 MPa/s the sandstone specimens can fail within 5-8 seconds. The induced specimen dilation is too rapid for Hoek cell or triaxial cell to

release the pressurized oil and maintain a constant confining pressure during loading. The excess oil pressure due to rapid dilation could lead to an error of the strength results.

4 TEST RESULTS

Figure 1 plots the axial stress-strain curves obtained from the uniaxial loading tests under various loading rates for the three sandstones. Despite the intrinsic variability among the specimens the curves tend to show loading-rate dependent behavior of the rocks. The higher the loading rates applied, the higher the rock strength and stiffness obtained. Figure 2 gives some examples of the triaxial compression test results for the loading rates ($\partial\sigma_1/\partial t$) of 0.01, 0.1, and 1.0 MPa/s for the PK sandstone. The tangent elastic moduli at 50% failure stress have been calculated from the measured stress-strain curves obtained from all uniaxial and triaxial loading specimens. The elastic moduli are plotted as a function of $\partial\sigma_1/\partial t$ in Figure 3. For all sandstones tested here the elastic modulus exponentially decreases with the applied $\partial\sigma_1/\partial t$, which can be best represented by a power equation: $E = \kappa (\partial\sigma_1/\partial t)^\xi$, where κ and ξ are empirical constants. Figure 3 gives numerical values for these constants. The average Poisson's ratios are 0.36, 0.38 and 0.15 for the PP, PW and PK sandstones, respectively. They tend to be independent of the loading rates. Post-test observations indicate that under confining pressures of 7 MPa or less, the specimens fail by a combination of compressive shear and splitting tension modes. Under the confining pressure of 12 MPa extension fractures dominate.

The maximum principal stresses at failure are plotted as a function of the minimum principal stresses (confining pressures) in Figure 4. Based on the Coulomb strength criterion the cohesion (c) and internal friction angle (ϕ) of the rocks have been calculated and presented in the figure. The loading-rate effect apparently acts at all magnitudes of the confining pressures. The failure envelopes clearly show that the failure stresses decrease with decreasing loading rates. The effect of the confining pressures on the loading-rate dependency of the tested sandstones remains inconclusive due to the relatively narrow range of the applied confining pressures and the intrinsic variations of the rocks.

5 DEVELOPMENT OF A STRENGTH CRITERION

The failure envelopes presented in Figure 4 are not directly applicable for a stability analysis of geological structures. This is primarily because the changes with time of the rock stresses during constructions or excavations may occur in all three principal directions. It is therefore necessary to develop a strength criterion that can incorporate the effects of the loading rates for the three principal stresses. In stead of a series of failure envelopes as given in Figure 4, a single failure envelope for each rock type would also be more practical for a stability analysis of in-situ rocks.

To examine the three-dimensional stresses at failure as affected by the loading rate, the second order of the stress invariants ($J_2^{1/2}$) at failure are calculated and presented as a function of the first order of the stress invariant or mean stress (J_1) in Figure 5. The failure envelopes in the $J_2^{1/2} - J_1$ diagram still show the effect of the loading rate. At the same J_1 a higher loading rate yields a greater $J_2^{1/2}$ value. This implies that the rate-dependent stiffness should also be considered in the derivation of a strength criterion.

An empirical relation is first proposed to represent the rock elastic modulus as affected by the stress rates along the principal directions. Assuming that the rocks are linearly elastic and isotropic the elastic modulus (E) is defined as:

Loading rate effects on strength and stiffness of sandstones under confinement

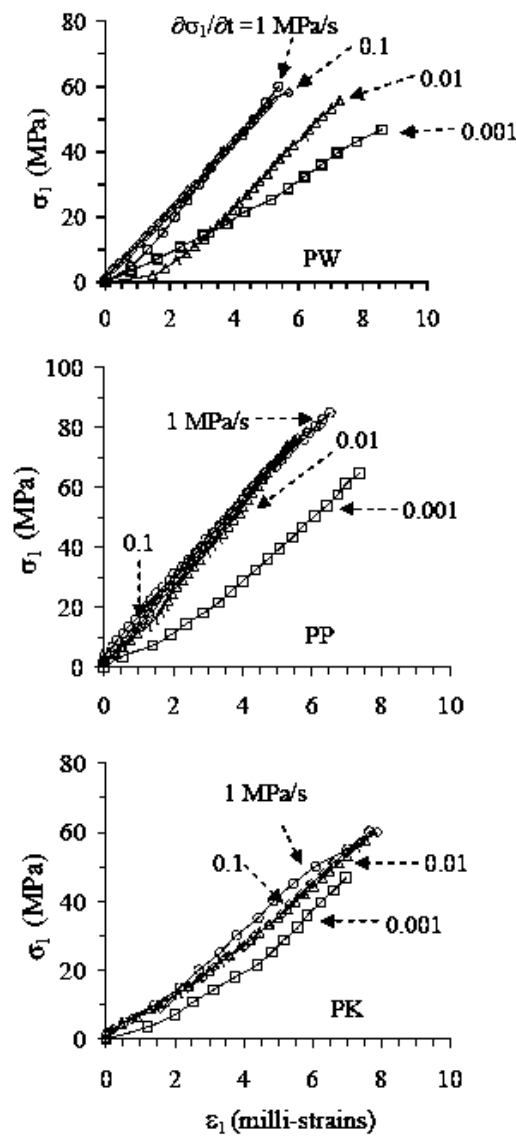


Figure 1. Uniaxial compressive strength testing results under loading rates varied from 0.001, 0.01, 0.1 and 1.0 MPa/s, for PW, PP and PK sandstones.

$$E = A (\partial J_2 / \partial t)^\beta \quad (1)$$

where A and β are empirical constants.

$$\partial J_2 / \partial t = (\partial / \partial t) (1/6) [(\sigma_1 - \sigma_2)^2 + (\sigma_2 - \sigma_3)^2 + (\sigma_3 - \sigma_1)^2] \quad (2)$$

For the uniaxial and triaxial stress conditions where the confining pressures ($\sigma_2 = \sigma_3$) are constant with time and the axial stress is increased at a constant rate ($\sigma_1 = \sigma_R t$), equation (2) can be simplified as:

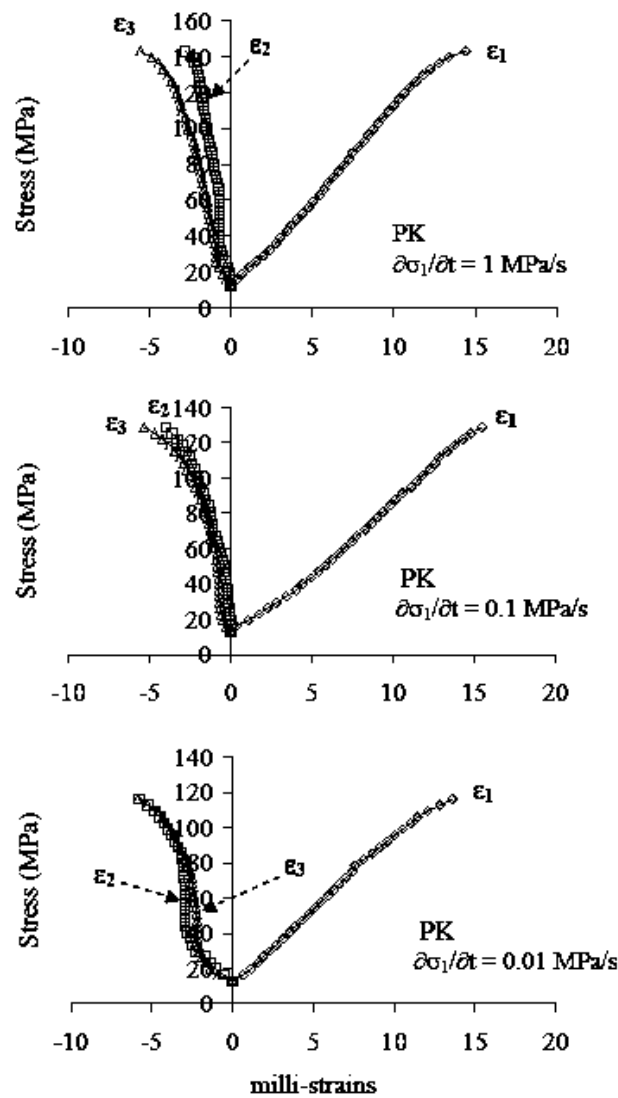
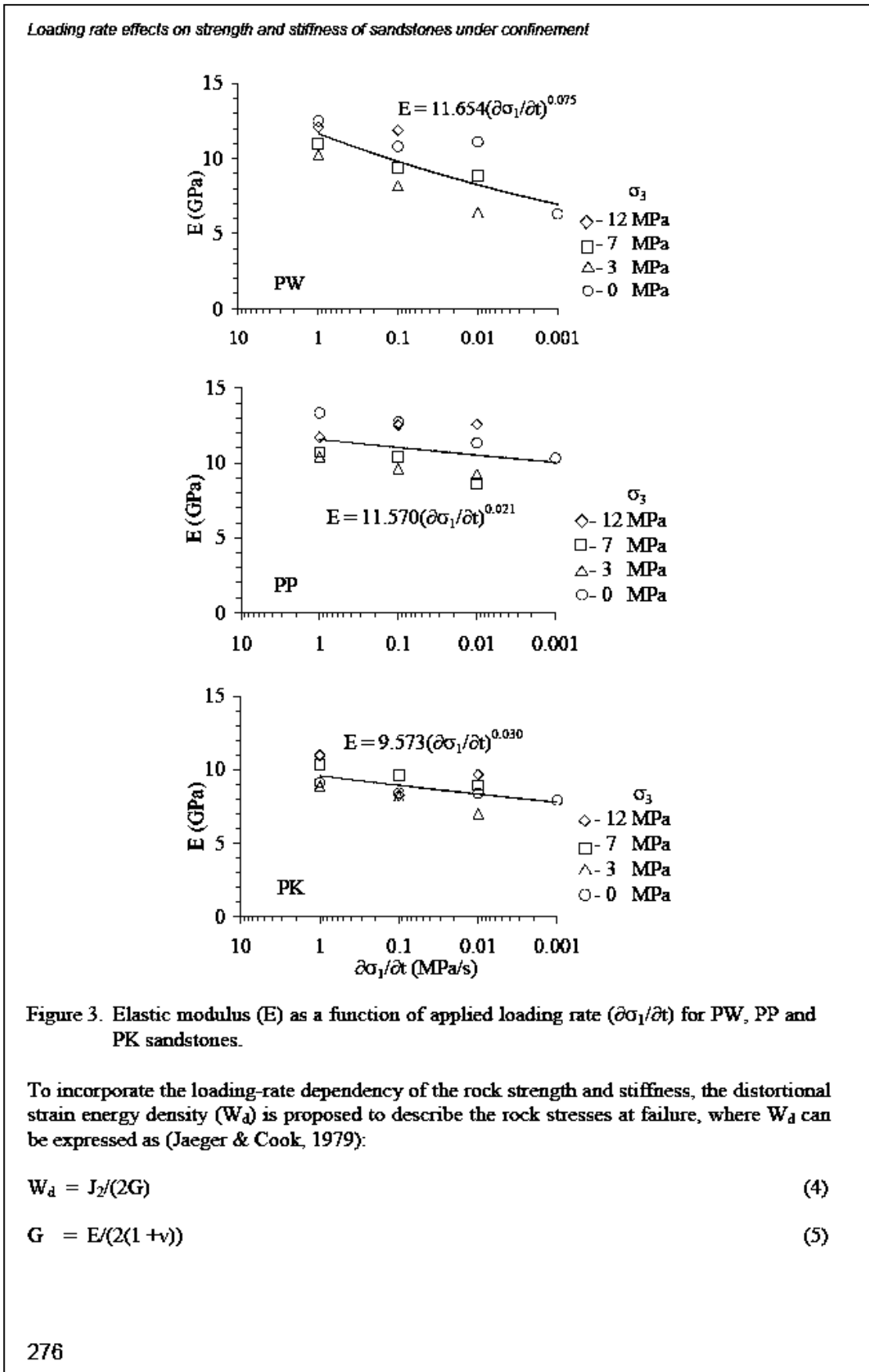


Figure 2. Examples of triaxial compressive strength testing results for PK sandstone with axial loading rates of 1, 0.1, and 0.01 MPa/s (from top to bottom).

$$\frac{\partial J_2}{\partial t} = \frac{2}{3} \sigma_R (\sigma_1 - \sigma_3) \quad (3)$$

where σ_R is the constant stress rate along the major principal direction (in MPa/s).

Figure 6 presents the rock elastic modulus (E) as a function of $\frac{\partial J_2}{\partial t}$ for all confining pressures, and lists the numerical values of the constants A and β for the three sandstones. The rock elasticity decreases exponentially with decreasing $\frac{\partial J_2}{\partial t}$. The exponent β indicates the slope of the curve on the semi-log scale while the constant A represents the rock elastic modulus at the stress invariant rate of $1.0 \text{ MPa}^2/\text{s}$.



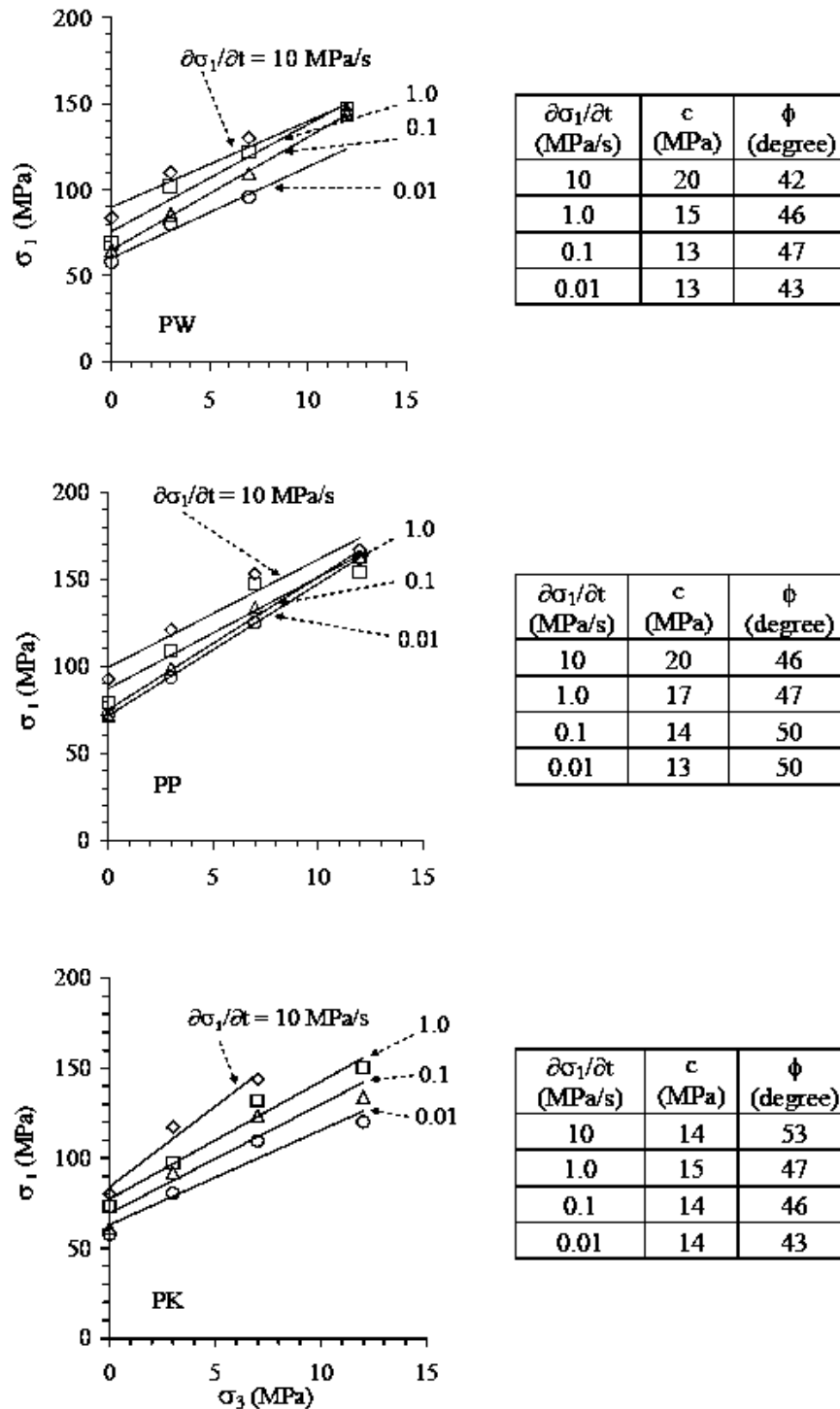


Figure 4. Maximum principal stress (σ_1) as a function of minimum principal stress (σ_3) at failure at various loading rates for PW, PP and PK sandstones.

Loading rate effects on strength and stiffness of sandstones under confinement

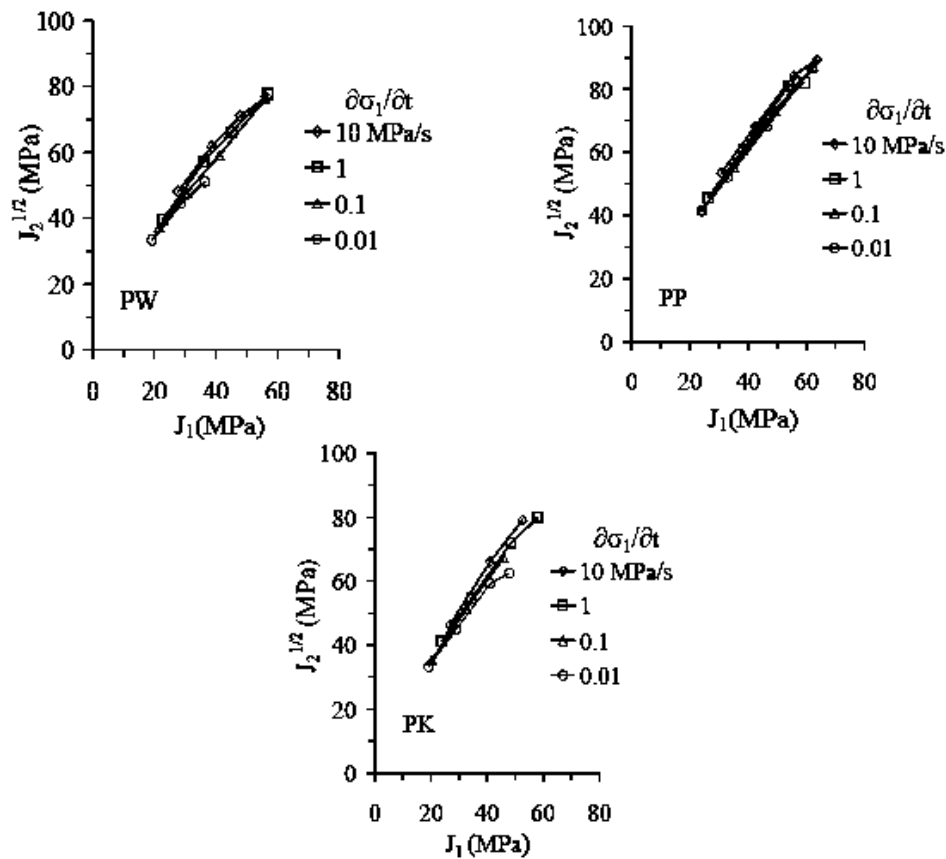


Figure 5. $J_2^{1/2}$ as a function of J_1 at failure for various loading rates for PW, PP and PK sandstones.

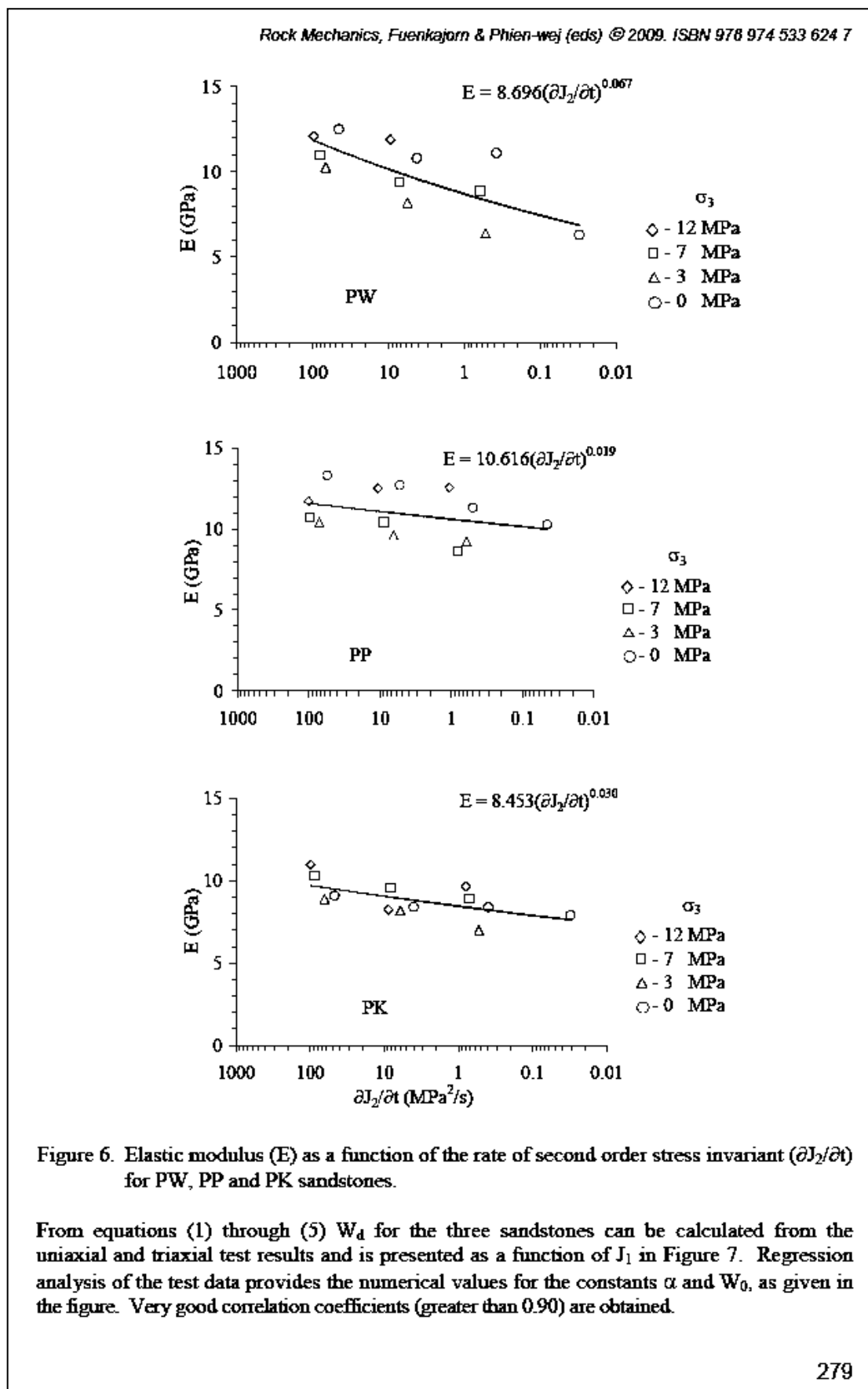
where G is the rock shear modulus which can be defined as a function of the loading rates along the principal directions by substituting equation (1) into equation (5), and assuming that the rock Poisson's ratio is independent of the loading rates. Equation (4) implies that W_d at failure for each rock type is constant under a given confining pressure. This means that as the loading rate decreases, the shear modulus G and the second order of the stress invariant J_2 at failure decrease with the same proportion.

Let's assume here that the effect of loading rate acts equally at all magnitudes of the mean stress (or first order of stress invariant, J_1). A strength criterion that implicitly incorporates the loading rate effect can therefore be presented as:

$$W_d = \alpha J_1 - W_0 \quad (6)$$

The constants α and W_0 depend on rock type, where α represents the slope of the failure envelope and W_0 is the intercept. The mean stress J_1 can be obtained from:

$$J_1 = (1/3) (\sigma_1 + \sigma_2 + \sigma_3) \quad (7)$$



Loading rate effects on strength and stiffness of sandstones under confinement

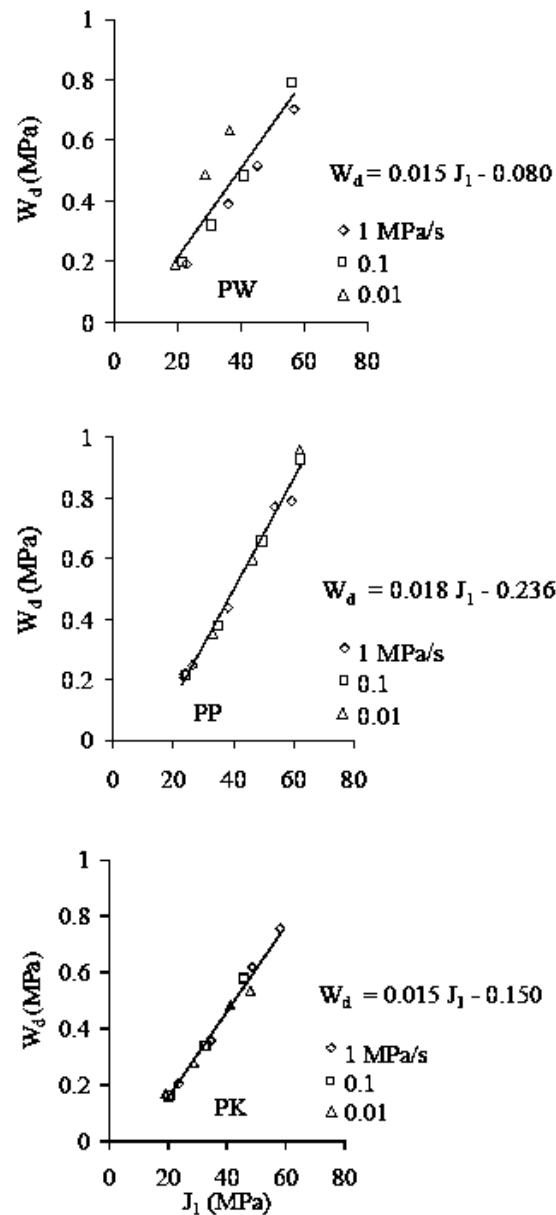


Figure 7. Distortional strain energy density (W_d) as a function of mean stress (J_1) for PW, PP and PK sandstones.

Here the loading rate effect on the rock elasticity has been incorporated into the proposed strength criterion by using equation (1). The loading rate effect on the failure stresses is considered by deriving the strength criterion in the form of the distortional strain energy density [equation (6)]. The proposed strength criterion is based on an assumption that under a given mean stress, the same distortional strain energy density is required to fail the specimen for each rock type. As a result a single failure envelope can represent the rock strengths under various loading rates and mean stresses.

6 DISCUSSIONS AND CONCLUSIONS

The proposed strength criterion, equation (6), can be applied to assess the stability conditions of any in-situ rock subjected to stress rates along the three principal directions. This can be accomplished by first performing uniaxial compressive strength tests of the rock under various loading rates. Assuming that the loading-rate effects act equally under all confining pressures, the elastic modulus can be defined as a function of $\partial J_2/\partial t$, i.e. by determining the empirical constants A and β in equation (1). A failure envelope ($W_d - J_1$ curve) can be constructed from the strength test data by using equations (4) through (6). Note that for other rocks the $W_d - J_1$ failure envelope may not be in linear form. For soft rocks under high confining pressures a non-linear relation may be used to fit the experimental results in the $W_d - J_1$ diagram. The W_d induced by the loading rates on the three principal stresses under an in-situ condition, probably predicted from numerical simulations, can then be compared against the criterion developed above. If the loading rates of the in-situ rocks are known for all three principal stresses, equation (2) should be used to determine $\partial J_2/\partial t$, and subsequently obtaining the elastic modulus as affected by the multi-axial loading rates.

It is concluded from this study that to assess the loading-rate dependency of dry and brittle rocks the strength criterion can be defined in terms of the distortional strain energy density (W_d) as a function of the mean stress (J_1) at failure. Here the proposed criterion can well describe the uniaxial and triaxial compressive strengths of the PP, PW and PK sandstones for the range of the loading rates from 0.001 to 10 MPa/s with the confining pressures up to 12 MPa. The criterion is based on an assumption that the loading rate effects act equally at all confining pressures. This results in a single failure envelope which is useful for predicting the strength of in-situ rocks subject to loading rates that are different from those used in the laboratory. The proposed strength criterion is applicable for the multi-axial stress rates induced simultaneously along the three principal directions of linearly elastic and isotropic rocks.

ACKNOWLEDGMENT

This research is funded by Suranaree University of Technology. Permission to publish this paper is gratefully acknowledged.

REFERENCES

- ASTM D 4543-85. Standard practice for preparing rock core specimens and determining dimensional and shape tolerances. *Annual Book of ASTM Standards*. Vol. 04.08. Philadelphia: American Society for Testing and Materials.
- ASTM D 7012-07. Compressive strength and elastic moduli of intact rock core specimens under varying states of stress and temperatures. *Annual Book of ASTM Standards*, Vol. 04.08. West Conshohocken: American Society for Testing and Materials.
- Aubertin, M., Li, L., & Simon, R., 2000. A multiaxial stress criterion for short- and long-term strength of isotropic rock media, *International Journal of Rock Mechanics and Mining Sciences*, 37: 1169-1193
- Blanton, T.L., 1981. Effect of strain rates from $10^{-2}/s$ to $10^1/s$ in triaxial compression tests on three rocks. *International Journal of Rock Mechanics and Mining Sciences & Geomechanics Abstracts*. 18: 47-62.

Loading rate effects on strength and stiffness of sandstones under confinement

- Chong, K.P., Harking, J.S., Kuruppu, M.D. & Leskinen, A.I., 1987. Strain rate dependent mechanical properties of western oil shale. *Proceedings of the 28th US. Rock mechanics Symposium*, Rotterdam: Balkema, pp. 157-164.
- Costin, L.S., 1987, Time-dependent deformation and failure, *Fracture Mechanics of Rock*, Barry Kean Atkinson, Editor, London: Academic Press, pp. 167-215
- Cristescu, N.D. & Hunsche, U., 1998, *Time Effects in Rock Mechanics*, New York: John Wiley & Sons.
- Daemen, J.J.K., 2009. On the importance, and difficulty, of dealing with the time dependency of engineered structures in, on, or with hard rock. *Proceedings of the Second Thailand Symposium on Rock mechanics*. March 12-13, 2009, Nakhon Ratchasima: Suranaree University of Technology.
- Farmer, I.W., 1983. *Engineering Behaviour of Rock*, second edition, London: Chapman and Hall.
- Hashiba, K., Okubo, S. & Fukui, K., 2006. A new testing method for investigating the loading rate dependency of peak and residual rock strength. *International Journal of Rock mechanics and Mining Sciences*. 43: 894-904.
- Ishizuka, Y., Koyama, H. & Komura, S., 1993. Effect of strain rate on strength and frequency dependence of fatigue failure of rocks. *Assessment and Prevention of Failure Phenomena in rock Engineering*. pp 321-327.
- Jaeger, J.C. & Cook, N.G.W., 1979. *Fundamentals of Rock Mechanics*. London: Chapman and Hall.
- Kohmura, Y. & Inada, Y., 2006. The effect of the loading rate on stress-strain characteristics of tuff. *Journal of the Society of Materials Science*. 55(3): 323-328.
- Kumar, A., 1968. The effect of stress rate and temperature on the strength of basalt and granite. *Geophysics*. 33(3): 501-510.
- Li, Y. & Xia, C., 2000. Time-dependent tests on intact rocks in uniaxial compression. *International Journal of Rock Mechanics & Mining Sciences*. 37: 467-475.
- Mosquera, M.J., Benítez, D. & Perry, S.H., 2002. Pore structure in mortars applied on restoration effect on properties relevant to decay of granite buildings. *Cement and Concrete Research*. 32: 1883-1888.
- Okubo, S., Fukui, K. & Qingxin, Q., 2006. Uniaxial compression and tension tests of anthracite and loading rate dependence of peak strength. *International Journal of Coal Geology*. 68: 196-204.
- Okubo, S., Fukui, K. & Jiang, X., 2001. Loading rate dependency of Young's modulus of rock. *Shigen-to-Sozai*. 117(1): 29-35.
- Okubo, S., Nishimatsu, Y. He, C. & Chu, S.Y., 1992. Loading rate dependency of uniaxial compressive strength of rock under water-saturated condition. *Journal of the Society of Materials Science, Japan*. 41(463): 403-409.
- Ray, S.K., Sarkar, M. & Singh, T.N., 1999. Effect of cyclic loading and strain rate on the mechanical behaviour of sandstone. *International Journal of Rock Mechanics & Mining Sciences*. 36: 543-549.
- Walsri, C., Poonprakon, P., Thosuwan, R. & Fuenkajorn, K., 2009. Compressive and tensile strengths of sandstones under true triaxial stresses. *Proceedings of the Second Thailand Symposium on Rock mechanics*. March 12-13, 2009, Nakhon Ratchasima: Suranaree University of Technology.
- Wang, X.B., 2008. Effect of loading rate on entire deformational characteristics of rock specimen. *Rock and Soil Mechanics*. 29(2): 353-358.
- Zhang, Z.X., Kou, S.Q., Yu, J., Yu, Y., Jiang, L.G. and Lindqvist, P.A., 1999. Effects of loading rate on rock fracture. *International Journal of Rock Mechanics and Mining Sciences*. 36: 597- 611.

BIOGRAPHY

Mr. Numchok Kenkhunthod was born on August 11, 1983 in Nakhon Ratchasima province, Thailand. He received his Bachelor's Degree in Engineering (Geotechnology) from Suranaree University of Technology in 2007. For his post-graduate, he continued to study with a Master's degree in the Geological Engineering Program, Institute of Engineering, Suranaree university of Technology. During graduation, 2007-2009, he was a part time worker in position of research assistant at the Geomechanics Research Unit, Institute of Engineering, Suranaree University of Technology. He has published one technical papers related to rock mechanics, titled **“Loading rate effects on strength and stiffness of sandstones under confinement”** published in the Proceeding of the Second Thailand symposium on rock mechanics, Chonburi, Thailand.